12-2004

Kinetics and Mechanism of the Catalysis of the Decomposition of Hydrogen Peroxide by Schiff Base Complexes of Copper(II).

Timothy Kum Beng
East Tennessee State University

Kinetics and Mechanism of the Catalysis of the Decomposition of Hydrogen Peroxide by Schiff Base Complexes of Copper(II)

A thesis
presented to
the faculty of the Department of Chemistry
East Tennessee State University

In partial fulfillment
of the requirements for the degree
Master of Science in Chemistry

---

by
Timothy Kum Beng
December 2004

Jeffrey G. Wardeska, PhD, Chair
Thomas T. -S. Huang, PhD.
Scott J. Kirkby, PhD.

Keywords: Copper-base adduct (CuB_2), Hydrogen peroxide, Copper(II) complexes, $[CuSALAD]_2.H_2O$, Catalase, Mononuclear, Binuclear.

ABSTRACT

Kinetics and Mechanism of the Catalysis of the Decomposition of Hydrogen Peroxide by Schiff Base Complexes of Copper(II)

By

Timothy Kum Beng

Spectroscopic studies have been used to describe the mechanism of the decomposition of hydrogen peroxide by solutions of a dimeric Cu(II) complex of a dissymmetric Schiff base, $[CuSALAD]_2.H_2O$, and imidazole or methyl substituted imidazoles, B, which form monomeric $CuSALAD.B_2$ complexes, in aqueous ethanol solvent. Freezing point depression and vapor pressure lowering studies were carried out to confirm the dimeric nature of the $[CuSALAD]_2.H_2O$ complex that had been previously reported. The stoichiometry of the $[CuSALAD]_2.H_2O$-imidazole equilibrium was extensively studied pointing to a 1:4 stoichiometry. The $CuSALAD.B_2$ adducts exhibited certain catalytic properties that mimic those of catalase enzymes. The different imidazoles were buffered to acidic, neutral, and basic pH media in order to investigate the pH effects of this reaction. Two charge transfer (CT) bands were observed near 420 and 450 nm upon addition of hydrogen peroxide to $CuSALAD.B_2$ solutions, and were associated with two proposed intermediates (CuBOOH and CuBOOCu). A mechanism consistent with these results has been developed. First order dependence of the rate on $CuSALAD.B_2$ was observed in the presence of excess $CuSALAD.B_2$ over hydrogen peroxide, whereas second order dependence was observed with the latter in excess. The CuBOOCu intermediate was unstable in the presence of EDTA, and a first order dependence of rate of formation of intermediate on both $CuSALAD.B_2$, and hydrogen peroxide was observed.

ACKNOWLEDGEMENTS

I thank and am forever indebted to my adviser, Dr. Jeffrey G. Wardeska, for his encouragement and guidance through many experiments, both fruitful and unproductive, his patience in dealing with an inexperienced laboratory student, his self-sacrifice by always putting my questions, issues, concerns, both academic and social above himself.

I thank Dr. Thomas T –S. Huang for helping me to undergo the ‘Grand Metamorphosis and Transition’ from being a cattle grazer, to marching slowly but steadily toward fulfilling my ultimate dream of becoming a professor in Chemistry. I also thank him for his time and devotion in training me on how to operate software that enabled me to treat all our kinetic data.

I thank Dr. Scott J. Kirkby for his motivation and willingness to serve on my graduate committee and for the special training he gave me on how to use the MathCAD software.

I thank all faculty and staff in the chemistry department at ETSU especially, Dr. Ismael Kady, Dr. Ray Mohseni, Dr. Richard Kopp, and Ms Susan Campbell for making my teaching experience such a wonderful and pleasurable one.

I thank all the Cameroonians at ETSU who helped to curb the home-sickness syndrome that was in me.

I thank my former and current Chemistry Laboratory students especially Martine Nkurunziza, Anna McClain, and Starla Kiser for helping me to discover my hidden talents.

CONTENTS

LIST OF TABLES

LIST OF FIGURES

CHAPTER 1
INTRODUCTION

Copper active sites play important roles in biological oxygen chemistry, such as reversible oxygen binding (hemocyanin), activation for substrate oxidation/hydroxylation (amine oxidase, galactose oxidase, tyroxinase), and reduction to water (ceruloplasmin). Copper enzymes often carry out such oxygen binding, activation and reduction. These enzymes exhibit unique spectroscopic features [1,8,9] which reflect novel electronic structures that can make key contributions to reactivity. The three multicopper oxidases are known to catalyze the 4-electron reduction of dioxygen to water. [2]

Studies of inorganic model systems have greatly contributed to the understanding of biological systems and much effort has been expended in trying to design and synthesize inorganic models that mimic the activity of catalase enzymes. Catalases are enzymes that catalyze the decomposition of hydrogen peroxide under certain biological conditions (i.e. low temperature, aqueous or lipid solvent systems, etc).

It is generally accepted that the first step in the metabolism of dioxygen in copper- based systems is the reaction of dioxygen with a coordinated copper(I) ion to produce a copper(II) peroxo or superperoxo intermediate. Most of these Cu/oxygen intermediates have been proposed, identified, and characterized [4-6] spectroscopically in biological Cu/oxygen chemistry. One of the structural motifs in biological Cu/oxygen intermediates is the side-on peroxide-bridged Cu(II) dimer present in the oxygenated form of hemocyanin. The side-on Cu_2 (O_2) core has characteristic spectral features including an intense charge transfer absorption band between 300-400 nm and a less intense-Laporte forbidden d-d transition around 570 nm that could be split due to Jahn Teller distortion. Because Cu(I), (d^{10}) complexes do not undergo d-d transitions, they do not show any peak in the 500-600 nm region.

Copper(II) complexes typically form four coordinate square planar and/or five coordinate square pyramidal to distorted trigonal pyramidal geometries and, which structure is assumed depends largely on the number, nature, and size of ligands coordinated to the Cu(II). The same factors can predict how fast or slow our reaction proceeds and the type of mechanisms involved. If three or fewer coordination sites are occupied, the peroxo prefers to bind in a "side-on" orientation with both oxygen atoms coordinated to both dimeric complexes [4]. If four sites are occupied, binding will occur in one of two possible "end-on" orientations. In one case, each oxygen atom will coordinate with separate copper ions and in the other case, both copper ions will coordinate with one oxygen atom while the other oxygen atom retains its hydrogen. Some of these binuclear and mononuclear intermediates have been proposed in this research project based on their peak positions and appearance or disappearance upon treatment with other reagents. The mononuclear category involves the peroxo Cu-OO, superoxo, and hydroperoxo CuOOH. The mononuclear reactive Cu/O_2 intermediate has been widely proposed to be CuOOH [1-4] with a charge transfer band between 400-500 nm.

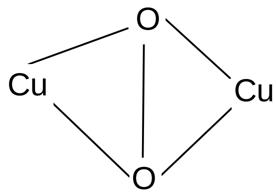

Structure 1: ‘side-on’ Cu_2O_2
Peak at 300 – 400 nm,
Present in hemocyanin.

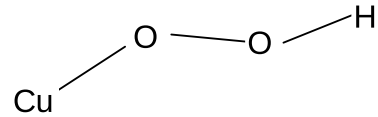

Structure 2: Hydroperoxo
Peak at 400 – 500 nm

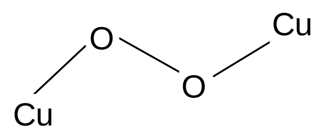

Structure 3: ‘end-on’ Cu_2O_2
Peak at 400-450 nm

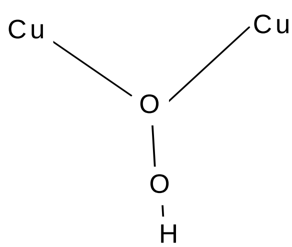

Structure 4: ‘end-on’ Cu_2O_2
Peak at 350 – 450 nm

Figure 1. Different Classes of Copper(II)-Peroxy Complexes.

In this study, the 500-600 nm peak is used to determine whether or not Cu(II) is reduced to Cu(I) during the catalysis of the decomposition of hydrogen peroxide. Another very useful test for Cu(I) in this study is its reaction with 2,2’-biquinoline producing a pink solution or complex. A negative test would suggest that copper remains in its +2 state after the reaction with H_2O_2 [6].

Because most of the Cu/oxygen chemistry that has been previously studied involved N-containing ligands coordinated to the Cu ion [7], our studies are designed to increase the knowledge of Cu/protein chemistry. In this regard the Schiff Base (SALAD) chosen for the study is made by reacting salicyaldehyde and (1S, 2S)-$(+)_D$-1-phenyl 2-amino 1, 3-propanediol, which acts as a tridendate ligand. The dimeric copper(II) complex, $[CuSALAD]_2$ is then prepared by mixing copper(II) acetate and the Schiff base in aqueous ethanol solvent. This complex when treated with imidazole and methyl imidazoles gives the Cu(II)-B adduct that is used as a catalyst for the decomposition of hydrogen peroxide. Imidazole and methyl imidazoles have been chosen as the bases of interest due to the important role that they play in biological systems when acting as ubiquitous ligands and also because they are readily available commercially and in different forms. Imidazole is a five-member nitrogen heterocycle and participates in dioxygen metabolism when copper is complexed by histidine-containing peptides [4]. Imidazole coordinates to the transition metals such as copper via one of the two nitrogen atoms residing in the five-member chain. It is present in proteins as part of the amino acid histidine chain, in nucleic acids structures as part of the purine ring of adenine and guanine, and as benzimidazole in the vitamin B-12 coenxyme.

Most of all the previous research in this area has involved adding dioxygen to copper(I) complexes and studying the reactions of dioxygen with copper ions as it progresses through the various peroxy and superperoxy forms ultimately to form water and oxygen.

Hydrogen peroxide (predominantly in the peroxide, HO_2^- form) can act as both an oxidizing and a reducing agent when involved in a redox reaction depending on the species with which it reacts. The thermodynamically favorable process is one with a positive electrode potential value.

$$HO_2^- + H_2O + 2e \longleftrightarrow 3\,OH^- \qquad E^o = -\,0.828\ V \tag{1}$$

$$HO_2^- + OH^- \longleftrightarrow O_2 + H_2O + 2e \qquad E^o = 0.076\ V \tag{2}$$

$$\Delta G = -\,nFE^0 \tag{3}$$

The free enthalpy change for the decomposition of two moles of a solution of hydrogen peroxide is -210.71 kJ. Many efforts have been made to clarify the autodecomposition of hydrogen peroxide, but these have not yet led to a satisfactory answer because of contradictions concerning the homogeneous or heterogeneous character of the decomposition, its pH dependence and kinetics, the rate influencing effects of possible impurities, and the mechanism of the reaction.

In this study, we investigate the changes in reactivity as the base is varied under two separate factors; steric effects (ImH *vs.* 2-MeIm) and number of available coordination sites (2-MeIm *vs.* 1-MeIm). Because reasonable rates are obtained with reproducible spectra for 2-MeIm than with the other methyl imidazoles, the former is almost exclusively used throughout the kinetic studies. We also report the effect of varying the concentration of CuSALAD.B_2 on rate and that of varying the concentration of hydrogen peroxide. Reaction conditions are chosen such that the dimeric Cu(II) complex and base are completely converted to the CuSALAD.B_2 adduct before the kinetic studies are performed. In this regard, a simple stoichiometric titration is carried out to determine the molar ratio of $[CuSALAD]_2$ to B required to completely drive the equilibrium to the right.

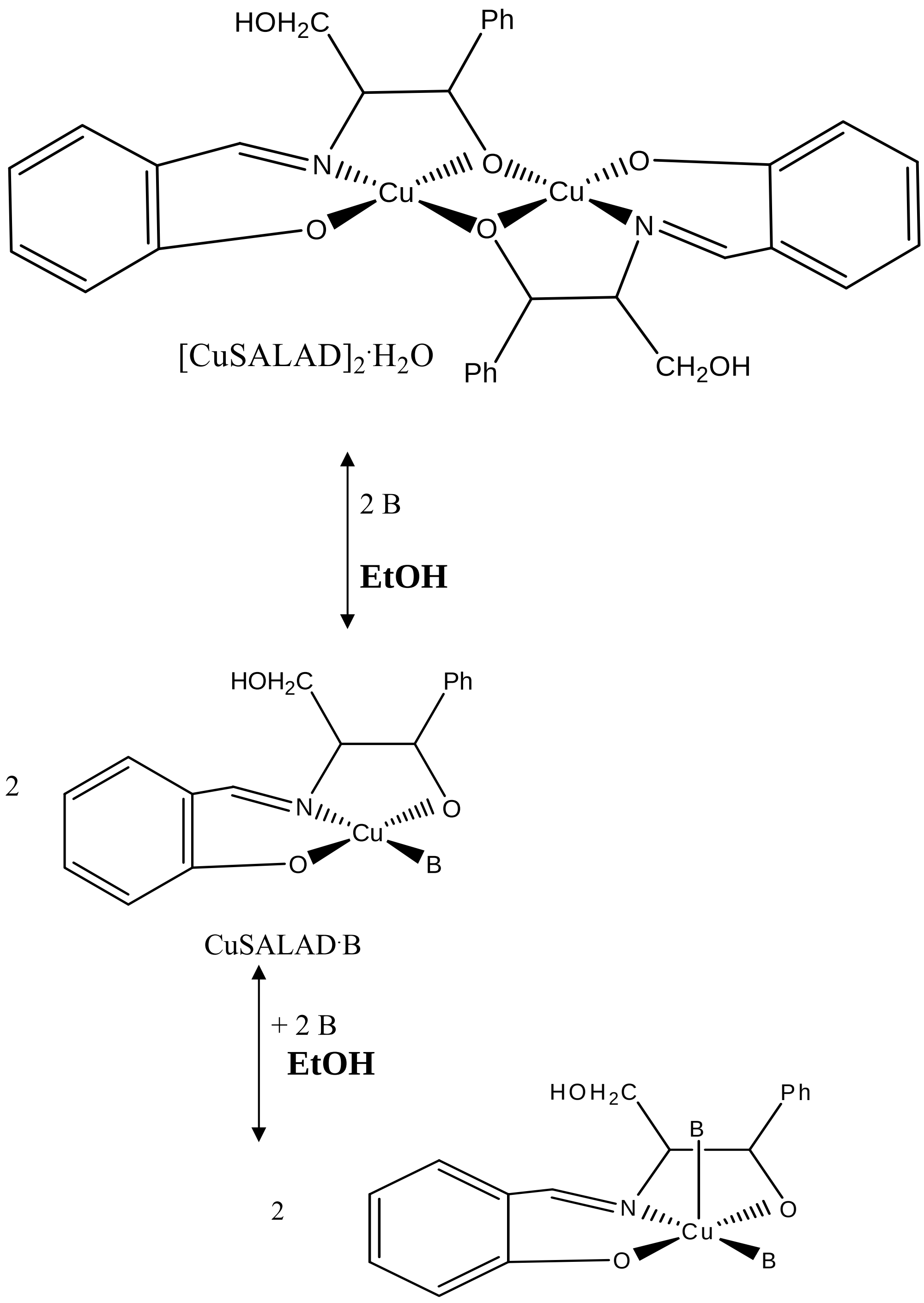

(Detailed Representation of equations 11 and 12, see page 54)

We also explore the concept of colligative properties of a solution in determining the molecular weight of the Cu(II) complex and confirm its dimeric structure that has been previously reported. Dilute solutions freeze at lower temperatures than the pure solvent upon cooling. When a non-volatile solute is dissolved in a solvent, however, the vapor pressure of the solvent is lowered, and equilibrium no longer exists at the freezing point of the solvent. Therefore, any solution of a solute in a solvent must have a freezing point lower than that of the solvent. The equilibrium approach is used to determine the freezing point depression which is the difference between the freezing point of pure liquid solvent and the freezing point of the solution.

The next focus of this research is to study the behavior of copper-peroxy reactions and to investigate the nature of peroxy-peroxy reactions initiated by their treatment with Cu(II) complexes. We report here the results of experimental work in which we sought further to elucidate the above mentioned issues or concerns**.** From a purely experimental point of view there are questions as to how rapidly these changes take place and how their rates depend on independent variables such as concentrations of reactants and catalysts, temperature and pressure, and the effect of soluble impurities. Sometimes it is found that the changes in the concentrations with time follow rather simple mathematical relations all the way to equilibrium. However, chemists are not satisfied with simply representing experimental results but want to understand what is going on in molecular terms. Even when there is a plausible mechanism for the changes that occur, there are questions as to why the steps in the mechanism have the rates they do and how the time course of the reaction could have been predicted in advance.

A kinetic study is carried out on the $CuSALAD.B_2$ adduct viewed as the catalyst in our studies in order to propose a reaction mechanism for its decomposition of hydrogen peroxide that is consistent with the observations made and results obtained. The progress of the reaction and the kinetic data were monitored using a CARY 1E UV-Visible Spectrophotometer via Electron Absorption Spectroscopy. Initial rate and Isolation Methods have been used to study the rate of formation of the intermediate around the 450 nm region.

CHAPTER 2
EXPERIMENTAL METHODS

Instrumentation, Glassware and Other Important Materials

A Cary 1E UV-Visible Spectrophotometer, pH meter, 1000 µL, 500 and 100 µL glass syringes, gauge syringe needles, 100 mL, 50, 25 and 10 mL volumetric flasks, 2 mL serological glass pipettes (graduated in 10 µL increments), 1.5 mL quartz crystal cuvettes were used in studying the kinetics of the decomposition of hydrogen peroxide. The standard Chemistry-Based Laboratory (CBL) unit,TI-89 calculator, Chembio software, Sartoris laboratory balance, temperature probes, pressure sensor, were among the hard and software tools that were used to determine the molecular weight of the dimeric copper(II) complex. A rubber stopper assembly, plastic hose, glass tube also constituted part of the experimental setup. Microsoft Excel (2003 version), Scientist, MathCAD, and other useful software packages were used in the treatment of the kinetic data. Other relevant materials such as beakers, Graduated cylinders, Pasteur pipettes, sample bottles, filter paper, watch glass, thermometers, and magnetic stirrers were used throughout this research project on multi occasions. The Cary 1E UV-Visible Spectrophotometer was also used to determine the molar stoichiometric ratio of dimer to base that was required to form the $CuSALAD.B_2$ adduct.

Reagent Grade Stock Chemicals

(1S, 2S)-$(+)_D$-1-phenyl-2-amino-1,3-propanediol obtained from Park-Davis company and recrystallized from ethanol, copper(II) acetate, reagent grade Salicylaldehyde (Sal), 95% ethanol, deionized water were used to synthesize the $[CuSALAD]_2$ complex. Reagent grade benzene and 100% USP grade ethanol were employed to determine the molecular weight of the dimer. Dilute and concentrated hydrochloric acid solutions were used in adjusting the pH of solutions during the kinetic studies and for cleaning the UV cells respectively. Hydrogen peroxide (30% and 3% USP grade) was obtained from commercial sources and used for the kinetic studies upon dilution to the required concentrations. Imidazole, 1-methylimidazole, 2-methylimidazole and 4-methylimidazole were the bases chosen in this study and used to convert the copper(II) complex into the CuB_2 adduct. Disodium ethylenediamminetetraacetate (Na_2H_2EDTA) was also added to the reaction medium in experiments designed to monitor the effect of impurities on the rate of peroxide decomposition. Methanol ($^{\cdot}OH$ scavenger) was added to the solution to help in detecting the presence of free radicals. Disodium (Na_2HPO_4) and monopotassium phosphate (KH_2PO_4) buffer and sodium hydroxide solutions helped in pH adjustments. Copper(II) nitrate was used to verify the role played by free copper ions in solution.

Experimental Procedure

Preparation of $[CuSALAD]_2.H_2O$

The detailed synthesis of $[Cu(II)SALAD]_2.H_2O$ has been previously described [3]. We report here a brief overview of the standard procedure used in synthesizing the Cu(II) complex. Generally speaking, salicylaldehyde was reacted with 1-phenyl-2-amino-1,3-propanediol while refluxing in ethanol to form the Schiff base, SALAD, a yellow crystalline product. Copper(II) acetate monohydrate, sodium acetate, and SALAD were each dissolved in an aqueous ethanol solvent and the solution was stirred to ensure completely dissolution. The mixture was then heated to near boiling, cooled, and the resulting green product was filtered. The product was recrystallized from a minimum amount of boiling ethanol and gravity filtered, air dried, and weighed. A quick UV absorption spectrum was taken using ethanol as the reference to assess the purity of the complex by comparing the molar extinction coefficient to that of its pure forms. The

$[CuSALAD]_2.H_2O$ complex has been well characterized and has been assigned the CAS Registry No. 80327-02-2. [3].

<u>Freezing Point Depression Measurements</u>

The freezing point measurements were made using a TI-89/CBL setup. A temperature probe was inserted into Channel 1 of the CBL unit which was then connected to a TI-89 calculator using the data-link cable. The CBL unit was turned on and the Chembio program was activated and used for data collection and processing. An ice-water bath was maintained at 0.00 $\pm$ 0.50 ^{o}C before 10.037g of the benzene solvent was weighed, put into a test tube, and clamped to a support. From the CHEMBIO ( ) program, the temperature probe was set up and the PERFORM VIEW option was selected in order to calibrate the probe. The temperature probe was then inserted into the ice-water bath until the CBL channel view voltage stabilized. The TRIGGER button was pressed on the CBL and the reference temperature (0 ^{o}C) was entered on the TI-89 calculator. The second calibration point was obtained by inserting the probe into the benzene solvent (at 20 $\pm$ 0.00 ^{o}C). Next a cooling curve to determine the freezing point of benzene was then obtained through the following steps: From the CHEMBIO screen, the options COLLECT DATA and TIME GRAPH were selected, '30 s' was chosen as the interval between readings and '30' as number of readings. The solvent was stirred periodically in order to ensure that the readings were uniformly recorded. Data collection and time graph were displayed after 900 seconds and the same procedure was repeated for solutions containing 10.037 g of benzene, 0.450 g and 1.000 g of $[CuSALAD]_2$ respectively.

Vapor Pressure Lowering Measurements

The vapor pressure lowering measurements were made using a TI-89/CBL/pressure sensor setup. A water bath was prepared and the temperature was allowed to stabilize at 25.0 ± 0.50 ^{o}C. The pressure sensor was connected to the CBL-TI-89 system and a rubber stopper assembly, containing a plastic hose, glass tube, and syringe, was connected to the pressure sensor. The CBL unit and calculator were turned on and the Chembio program was enabled. The temperature and pressure probes were set up and calibrated before the CBL and calculator were ready for data collection. To take a reading of the atmospheric pressure, the side valve stem of the 3-way valve was opened to the atmosphere. A stoppered 125 mL Erlenmeyer flask containing 2.0 mL of the ethanol solvent that was injected into the flask by means of a syringe was completely immersed in the water bath. The two-way valve was then closed and the stem leading to the reaction system was opened to obtain the solvent vapor pressure. When equilibrium between vapor and liquid ethanol was reached after about 10 minutes, the value for the pressure was recorded. The same procedure was repeated using 0.500 g of $[CuSALAD]_2$ and 2.0 mL of ethanol and the pressure value was also recorded. The temperature was then varied to study the variation of vapor pressure with temperature for the $[CuSALAD]_2$ solution.

Determination of Dimer/Base Stoichiometry

A solution containing 0.011g of $[CuSALAD]_2$ dissolved in 10 mL of ethanol (corresponding to 1.61 * 10^{-5} moles or 0.00161 M) was prepared and a 5 mL portion was used for the titration. Similarly, 0.245 g of 2-MeIm was dissolved in 10 mL of ethanol (corresponding to 0.00298 moles or 0.289 M solution) and incremental portions were added to the conical flask containing the $[CuSALAD]_2$ solution. The effect of the incremental addition of base into the $[CuSALAD]_2$ solution was monitored by the change in absorbance at 570 nm. The absorbance of the free $[CuSALAD]_2$ solution was first measured before incremental microliter portions of the 2-MeIm were added and repeated measurements taken after increments. As soon as the absorbance values started to decrease (after addition of more than 100 μL of 2-MeIm), the reaction was thought to have reached saturation and data collection was stopped. The absorbances were then corrected for blank and dilution, before the ratio of 2-MeIm to $[CuSALAD]_2$ was computed.

Preliminary Qualitative Tests

Previous kinetic studies involving $[CuSALAD]_2$-Im and hydrogen peroxide suggested that the progress of the reaction could be monitored via spectroscopic techniques by tracking the spectrally active intermediate around the 450 nm region of the spectrum. The challenge was therefore to optimize reaction conditions and obtain explicit and reasonable spectra. In this regard a series of qualitative tests were performed and the different optimum concentration ranges for the different species present were determined. The imidazole and methyl substituted imidazoles were kept in excess over the $[CuSALAD]_2$ to ensure complete conversion of the $[CuSALAD]_2$ into the $CuSALAD.B_2$ adduct. To do this, the molar concentration of the base was maintained at a 20- or higher- fold excess over $[CuSALAD]_2$. The tests involved the use of various concentrations of $[CuSALAD]_2.H_2O$, imidazole derivatives and initial hydrogen peroxide levels. The different imidazoles used in the research study were; 2-methylimidazole (2-MeIm), 1-methyimidazole (1-MeIm), imidazole (ImH), and 4-methylimidazole (4-MeIm). Aqueous ethanol solvent mixtures (70/30 and 60/40) was prepared by mixing different amounts of pure ethanol and deionized water. Tests using ethanol only as a solvent were also performed to monitor the effect that water has as a solvent in this study. Typically the $[CuSALAD]_2.H_2O$ gave a bright green solution when dissolved in the solvent but the $CuSALAD.B_2$ (CuB_2) complexes gave a bluish-purple type color especially with ImH, 4-MeIm and 1-MeIm upon standing. The initial hydrogen peroxide concentrations ranged from 0.0440 – 0.880 M with a maximum of 10 μL injected during each kinetic run. The initial $[CuSALAD]_2$ concentration ranged from 0.000100 – 0.00400 M whereas the initial base concentration ranged from 0.0100 – 0.0800 M.

A spectrum of a 0.00200 M CuB_2 solution with a 60/40 aqueous ethanol mixture as the reference cell was obtained and the peak around 570 nm was used to determine and confirm the oxidation state of copper in the CuB_2 adduct by comparing it to the spectrum obtained after two hours of elapsed time in the presence of H_2O_2.

The Effect of pH

The effect of pH on the rate of formation of the spectrally active intermediate at 445 nm was investigated by buffering the base, 2-MeIm to acidic, neutral, and basic pH ranges. This was done by using the phosphate buffer together with hydrochloric acid and sodium hydroxide solutions before injection of H_2O_2. The pH meter was used to measure the pH of the solution which was eventually adjusted to the required pH. Pre-calculated ratios of KH_2PO_4 and

Na_2HPO_4 were used to obtain the pH values of interest, (6.5, 7.7, and 8.5) which were slightly adjusted with solution of 3 M HCl or 6 M NaOH.

Kinetic Studies

Initial Rates Method: Initial rate studies were used to monitor the rate of formation of the suspected intermediate around 450 nm. A representative procedure for measuring the initial rate was as follows: A solution containing 1.5 mL of 0.00800 M [CuSALAD.(2-MeIm)$_2$]was put in a cuvette prior to the injection of 10.0 microliters of 0.044 M H_2O_2. The solution was then stirred with a syringe for 5 seconds to ensure that different components were completely mixed. The Cary 1E UV-Visible Spectrophotometer chart was started immediately after the injection of H_2O_2.The parameters were adjusted such that the maximum absorbance was 2.000 and the wavelength was fixed at 445 nm. The progress curve was obtained for over 1 hour of elapsed time and the first 2 minutes of the reaction were plotted on Excel 2003 and the slopes approximated as the initial rates of formation of the 445 nm intermediate.

Isolation Method: The Isolation method, otherwise known as Flooding Technique, was used to study the progress of the hydrogen peroxide decomposition reaction. The concentration of H_2O_2 was maintained at a 10- or higher fold excess over that of CuSALAD.B_2 such that changes in rates were assumed to be only due to changes in the concentration of CuB_2.A solution containing 0.000400 M CuB_2 and 0.00400 M H_2O_2 was used in one case and 0.00240 M EDTA was added to the reaction mixture in the other case. In both cases, the progress of the reaction was monitored for 60 minutes at 445 nm. The reference solution was made identical to the sample solution except that it didn't contain the hydrogen.peroxide.

Curve fitting was used to analyze data obtained from the Isolation method. A kinetic scheme which obeyed the behavior of our system was devised and was used to compute the values of the concentration of the intermediate.

$$A \longleftrightarrow B \qquad k_f, k_r \tag{4}$$

$$B \longrightarrow C \qquad k_d \tag{5}$$

k_f represents the forward rate coefficient, k_r = reverse rate coefficient and k_d = dissociation rate coefficient, The catalyst CuB_2 is represented by A, B stands for the proposed intermediate CuBOOH, and C represents either the product or a short-lived intermediate that immediately decomposes to form the product(s) of the reaction. The above scheme was used to solve for the concentration of B at any time, t, during the course of the reaction. After solving for [B], the following equation was obtained (See Chapter Four section for more detail).

$$[B] = \frac{k_f [A]_0 \{\exp(-k_f t) - \exp(-(k_r + k_d)t\}}{k_d + k_r - k_f} \tag{6}$$

The squares of differences between the experimental and calculated values of [B] were computed and added up to one value. The different rate coefficients were defined on using Excel 2003, under ‘Solver’. Guess values were chosen for the rate parameters and the sum of the deviations was selected on the spread sheet. After defining the limits of the guess values the equation was solved for different values of [B]. The guess values were repeatedly adjusted until the best possible fit between experimental and calculated values of B was obtained. ‘Solver Statistics’ was chosen under the ‘Add-on’ option in Excel 2003 and used to obtain the standard deviation and correlation coefficient of the different data. The two plots were generated and the same procedure repeated for different initial concentrations of CuB_2.

The Effect of EDTA

An absorption spectrum was obtained (from 400-700 nm) for a 0.00400 M $[CuSALAD]_2$-2-MeIm solution before the addition of a 0.00240 M solution of sodium ethylenediamminetetraacetate (Na_2H_2edta) and the changes in spectra and colors of the solutions were noted. Another spectrum was then obtained (from 400-460 nm) upon injection H_2O_2 in the presence and absence of EDTA and the progress of the intermediates was monitored. The spectra of the CuB_2 and CuB_2/EDTA solutions were taken to see if the EDTA, in addition to complexing the free copper ions or copper ions in the form $[Cu(2\text{-}MeIm)_2]^{2+}$in solution, also reacted with the CuSALAD.B_2. The color of the CuSALAD.B_2/EDTA solution was noted and compared with that of the EDTA-free solution.

A solution containing 0.00200 M copper(II) nitrate was also prepared and 0.10 mL of it was added to 1.0 mL of a 0.00400 M solution of the CuB_2 adduct. To verify that EDTA slowed down the rate of the decomposition of hydrogen peroxide by tying up one of the active species, possibly the free Cu(II) ions or $[Cu(2\text{-}MeIm)_2]^{2+}$ in solution, it was necessary to understand the role played by Cu(II) ions during the catalysis process. To do this, a spectrum of the CuB_2/H_2O_2 intermediate at 445 nm was obtained and then compared with that in the presence of $Cu(NO_3)_2$.

In an attempt to answer the question regarding the oxidation state of copper after the reaction, a spectrum of a 0.00800 M CuSALAD.B_2 was taken prior to the addition of H_2O_2 and after the addition of a 0.00440 M H_2O_2 solution when two hours of the reaction time had elapsed.

The solutions were also tested with 2, 2'-biquinoline and the color was noted. An absorption spectrum from 300-400 nm for the suspected side-on Cu_2O_2 binding was taken.

The Effect of Methanol

A solution of methanol was used to investigate the effect of free radicals ($\cdot OH$) on the catalytic decomposition of H_2O_2 by the CuB_2 complex. Its concentration was maintained at about 0.00200 M. Methanol is noted for its ability to scavenge hydroxyl radicals in solution. The idea therefore was that if the mechanism of the decomposition of hydrogen peroxide by the CuB_2 complex proceeded via a free radical pathway, the addition of modest quantities of methanol would slow down the rate tremendously or completely stop the progress of the reaction as a whole. In this regard, 1.0 mL of a 0.00400 M solution of CuSALAD.(2-MeIm)$_2$ was used and its absorption (445 nm) spectrum was obtained and then compared with that obtained from the mixture of 0.10 mL of 0.00200 M and 1.0 mL of 0.00400 M solutions of methanol and CuSALAD.(2-MeIm)$_2$ respectively.

CHAPTER 3
DATA AND RESULTS

Table 1 provides the results obtained from the experiment conducted in order to determine the molecular weight of $[CuSALAD]_2.H_2O$ by the freezing point depression technique in an attempt to confirm its previously reported dimeric structure.

Table 1**.** *Determination of the Molecular Weight of [CuSALAD]$_{2.}$ by Freezing Point Depression*

w_1 in grams	10.037	10.037
w_2 in grams	0.450	1.000
Freezing Temp of solvent, T_o (^oC)	5.545	5.545
Freezing Temp of solution, T_s (^oC)	5.234	4.923
K_f = molal freezing-point depression constant	5.0727	5.0671
Lit K_f ($^oCmol^{-1}$) (for T_f = 5.530^{o}C)	5.120	
M.W(g/mol)	731	814
Calculated M.W	683	

The different symbols used in the table are defined below.

w_1 = mass of solvent (benzene), w_2 = mass of $[CuSALAD]_2.H_2O$,

$$K_f = \frac{MRT_0^2}{\Delta H_{fus}} \tag{7}$$

$\Delta T_f = T_o - T_s$, M = molar mass of benzene, R = molar gas constant,
ΔH_{fus} is change in standard enthalpy of fusion of liquid benzene.

$$M_2 = \frac{1000 \times w_2 \times K_f}{w_1 \times \Delta T_f} \tag{8}$$

All the experiments were duplicated and the typical reproducibility of data was within 3%. The solutions were assumed to obey Raoult's Law, and the concordance of theory and experiment was more appreciable. The molal freezing-point depression constant was found to vary with the concentration of the solute with near dilute solutions giving more accurate results (see Table 1).

Table 2. *Determination of Molecular Weight of $[CuSALAD]_2$ by Vapor Pressure Lowering*

Atmospheric pressure (mmHg)	722
Room temperature (Kelvin)	293.8
Density of ethanol solvent (g/mL)	0.7893
Mass of $[CuSALAD]_2.H_2O$ (g)	0.500
Volume of ethanol (mL)	2.0
Pressure of ethanol (mmHg)	770
Pressure of solution (mmHg)	769
P^o (mmHg) ($P_{ethanol}$-P_{atm})	48
P^s (mmHg) (P_{soln}-P_{atm})	47
Extent of vapor pressure lowering (P^o-P^s)	1
M_2 (expt) in g/mol	700
M_2 (calculated from formula) in g/mol	683

Data obtained from experiments designed for the determination of the molecular weight of $[CuSALAD]_2.H_2O$ by the vapor pressure lowering technique are represented in Table 2.

$$M_2(\exp t) = \frac{M_1 \times P^0 \times W_2 \times [1 - \Delta P / P^0]}{W_1 \times \Delta P} \tag{9}$$

$\Delta P = P^o - P^s$, W_1 = mass of ethanol used = density/volume of ethanol used,

M_1 = molecular weight of ethanol (46.07 g/mol), W_2 = mass of analyte used. The solution was assumed to obey Raoult's Law for both liquid and vapor phases. The experimental value (700 g/mol) for the molecular weight of the complex agreed closely with the calculated value from atomic data (683 g/mol) within experimental error, and the extent of vapor pressure lowering was reasonably low (1.0 mmHg) as predicted from Raoult's law.

Appendix A shows the results of the spectrometric titration carried out to determine the molar stoichiometric ratio of $[CuSALAD]_2$ to 2-MeIm. Figure 2 shows a graphical representation of the results obtained. There was a definite break when 4 moles of base were added to 1 mole of the dimer suggesting a 1 : 4 (dimer : base) stoichiometry. (See figure 2). Previous experiments in which the intensity of the epr signal of the Cu(II)-B adducts were monitored showed identical results [3]

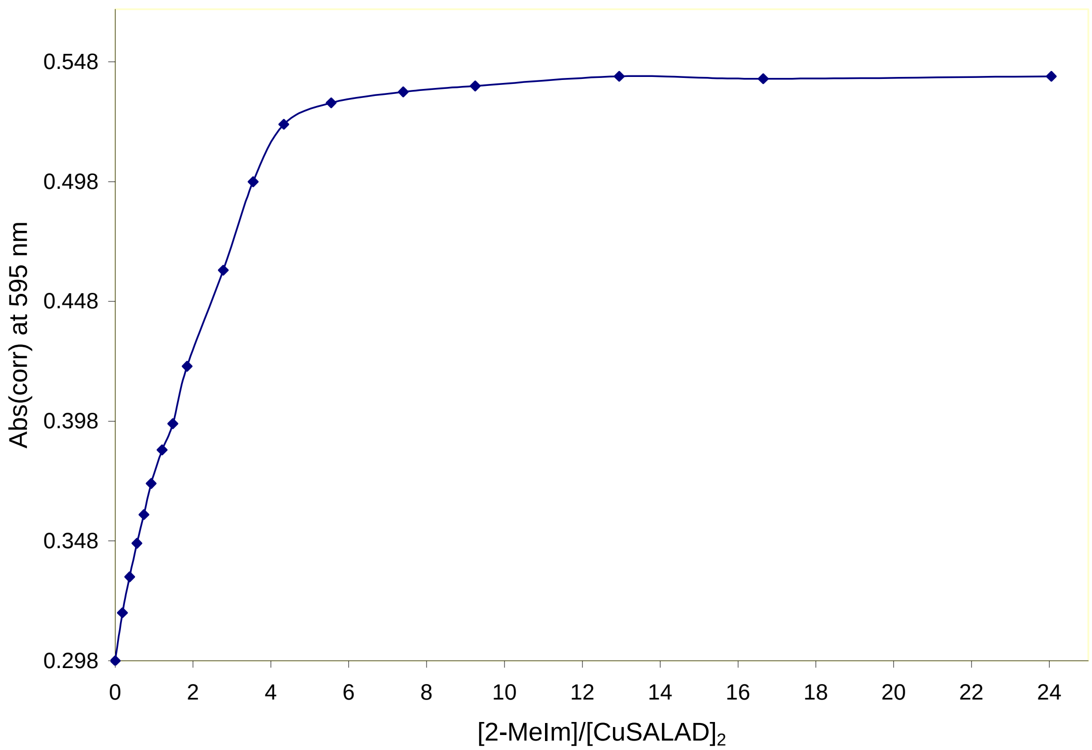

Figure 2. Determination of the $[CuSALAD]_2$: 2-MeIm Stoichiometry

(Data in Appendix A, page 67), [2-MeIm] = 0.289 M corrected for dilution $[[CuSALAD]_2]$ = 0.00161 M corrected for dilution. The absorbance values were corrected for both blank and dilution.

Kinetics of the Catalytic Decomposition of Hydrogen Peroxide

Most of the rates reported here are initial rates developed by measuring the increase in absorption of the 445 nm CT band as a function of time for 2 minutes of the reaction. Therefore, the rate laws are initial rate laws, and all concentration dependences are expressed in terms of *initial* concentrations. Reaction of aqueous ethanol solutions of $CuSALAD.B_2$ with hydrogen peroxide resulted in noticeable color changes of the solution from bluish-purple through greenish yellow to yellow, and eventually back to bluish-purple. A gas was evolved as the reaction involving the decomposition of hydrogen peroxide continued.

The progress of the formation and decay of the intermediates in the absence of EDTA was monitored and an absorption spectrum was obtained. Figure 3 shows a typical spectrum in which two intermediates, one around 450 nm and the other around 420 nm, are observed. As the reaction between the CuB_2 adduct and H_2O_2 progressed, the intensity of the 418 nm CT band increased but that of the 445 nm CT decreased.

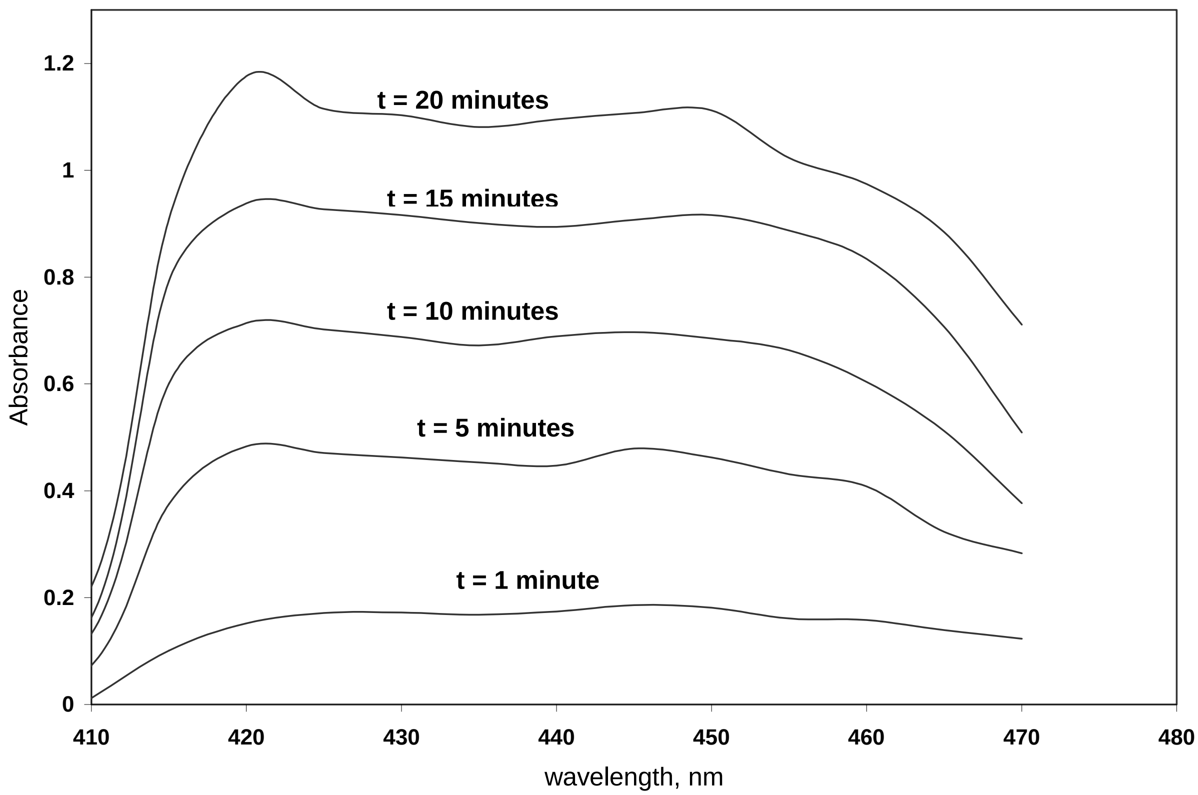

Figure 3. Spectra for the Reaction of $CuSALAD.B_2$ and H_2O_2 in the Absence of EDTA

$[H_2O_2]_0 = 4.36 * 10^{-4}$ M, $[CuSALAD]_2.H_2O]_0 = 1.19 * 10^{-3}$ M, $[2\text{-MeIm}]_0 = 5.54 * 10^{-3}$ M

In order to investigate the role played by EDTA in the reaction, 0.05 mL of a 0.00200 M solution of EDTA was added to 1.0 mL of a 0.00800 M solution of CuB_2. EDTA was then used to look for trace $Cu^{2+}(aq)$ that might also catalyze the hydrogen peroxide decomposition reaction. The absorption spectra obtained for the EDTA-free and EDTA-containing solutions are represented in figure 4.

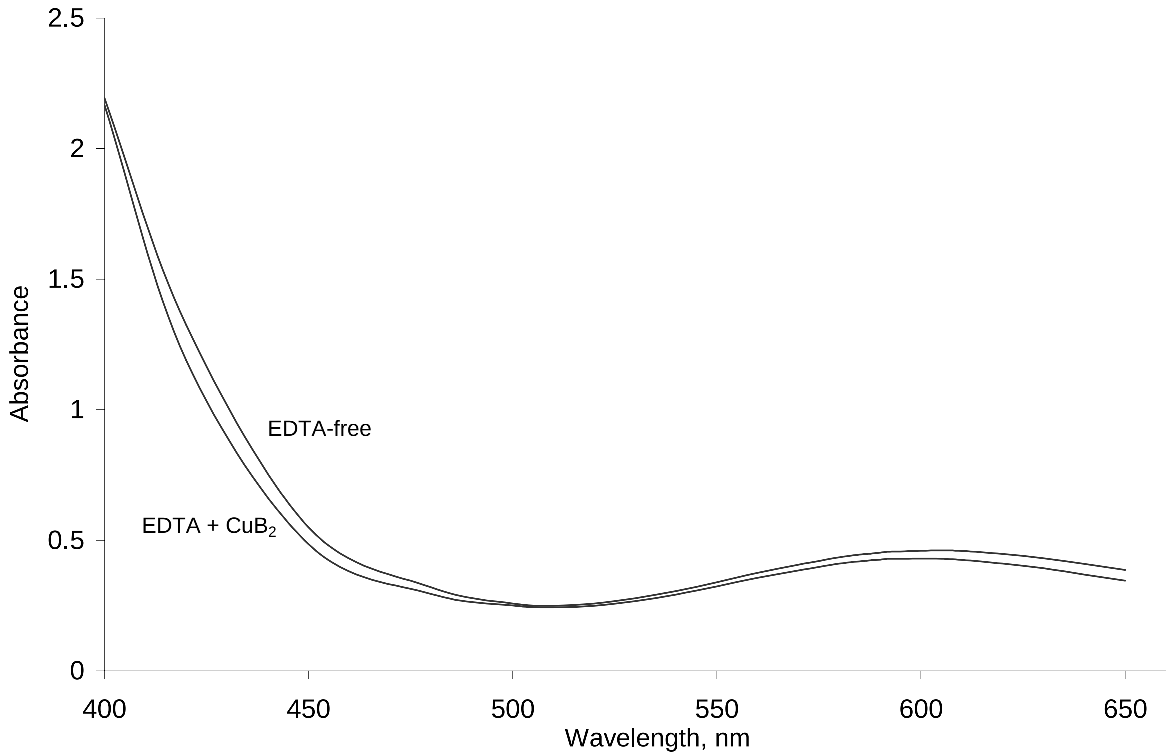

Figure 4. Spectra for the CuB_2 and CuB_2/EDTA Systems Showing the Consistency in Appearance of the 595 nm d-d Absorption peak

The effect due to dilution of the CuB_2 595 absorption peak was calculated and used to interpret the spectra. The solutions were maintained at a constant volume of 1.05 mL.

$[[CuSALAD]_2.H_2O]_0 = 0.0040$ M, $[CuB_2]_0 = 2 * [Cu_2]_0$, $[EDTA]_0 = 0.00200$ M. The change in absorbance was approximately four times the change in concentration and the 595 nm peak was 6% diluted.

The progress of the formation and decay of the intermediates in the presence of EDTA was monitored and an absorption spectrum was obtained. Figure 5 shows a typical spectrum in which two intermediates, one around 450 nm and the other around 420 nm, are observed in the first 5 minutes. As the reaction between the CuB_2 adduct and H_2O_2 progressed, the intensity of the 418 nm CT band decreased significantly and was completely lost after 10 minutes of elapsed time but that of the 445 nm CT grew rapidly.

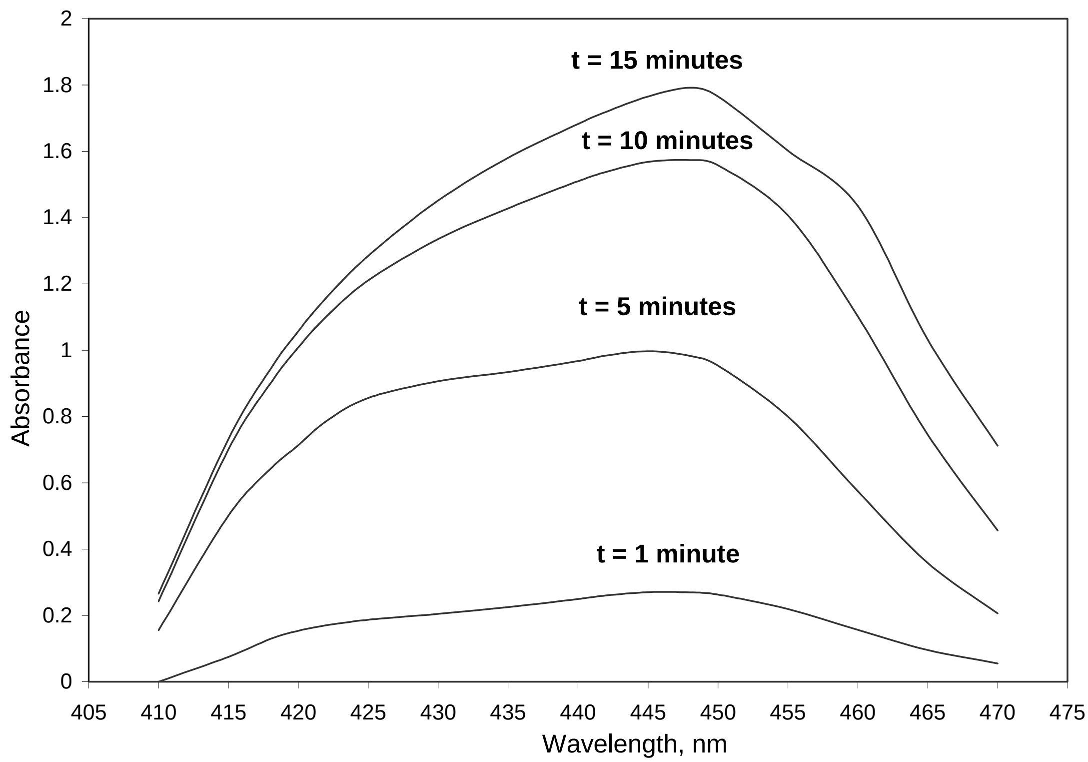

Figure 5. Spectra for the Reaction of CuSALAD.B_2 with H_2O_2 in the Presence of EDTA

$[H_2O_2]_0 = 4.36 * 10^{-4}$ M, $[CuSALAD]_2.H_2O]_0 = 1.19 * 10^{-3}$ M, $[2\text{-MeIm}]_0 = 5.54 * 10^{-3}$ M, $[EDTA]_0 = 2.00 * 10^{-3}$ M

Appendix B provides a tabular representation of data showing the effect of varying the different imidazoles and methyl substituted imidazoles on the rate of formation of the 445 nm intermediate.

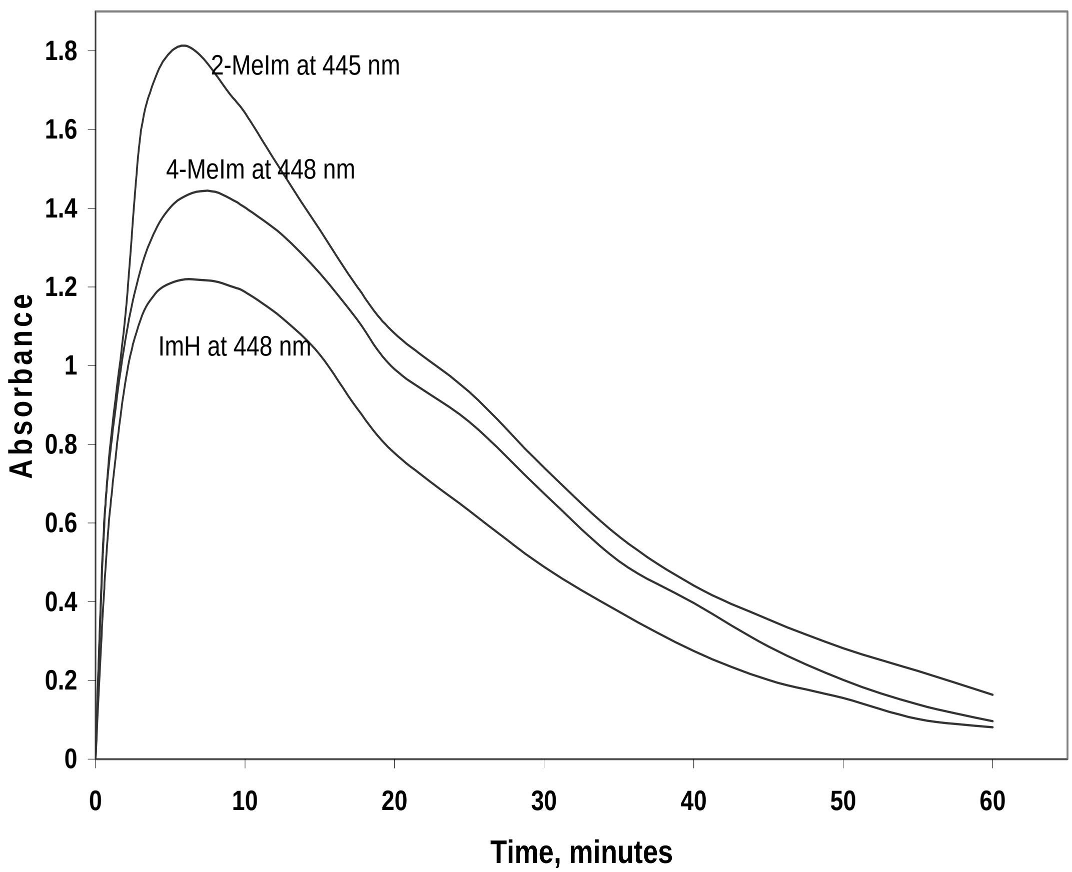

Figure 6. Rate Dependence on the Different Imidazoles and Methyl Substituted Imidazoles

$[[CuSALAD]_2.H_2O]_0$ = 0.00400 M, $[H_2O_2]_0$ = 0.00130 M, $[B]_0$ = 0.0800 M.

Table 3. *Initial Rates vs. Type of Imidazole Derivative*

Imidazole derivative	Initial rate, (10^{-3} s^{-1})	pKa
Imidazole (ImH)	5.70	6.90
2-Methylimidazole (2-MeIm)	6.82	7.77
4-Methylimidazole (4-MeIm)	6.32	7.35

It was observed that the peak intensities (see Figure 6) and initial rates of formation of the spectrally active intermediate (see Table 3) were highest in the case of 2-MeIm. It was equally relatively easy to reproduce data when 2-MeIm was used than with the other two bases. After the formation of the CuSALAD.B_2 adducts with the different bases, it was observed that the colors of the solutions were slightly different. While the ImH and 4-MeIm gave significant purplish-blue solutions, solutions of 2-MeIm were more bluish than purplish. All kinetic studies were subsequently carried out using 2-MeIm as the base of choice.

The order of increase in the initial rate of formation of intermediate was directly reflected in the order of pKa values for the different imidazoles. This led to the investigation of the effect of pH on the rate of formation and decay of the intermediate at 445 nm using 2-MeIm as the base. Data representing the effect of variation of pH are shown in Appendix F and Figure 7 shows a plot of the results obtained from the pH measurements.

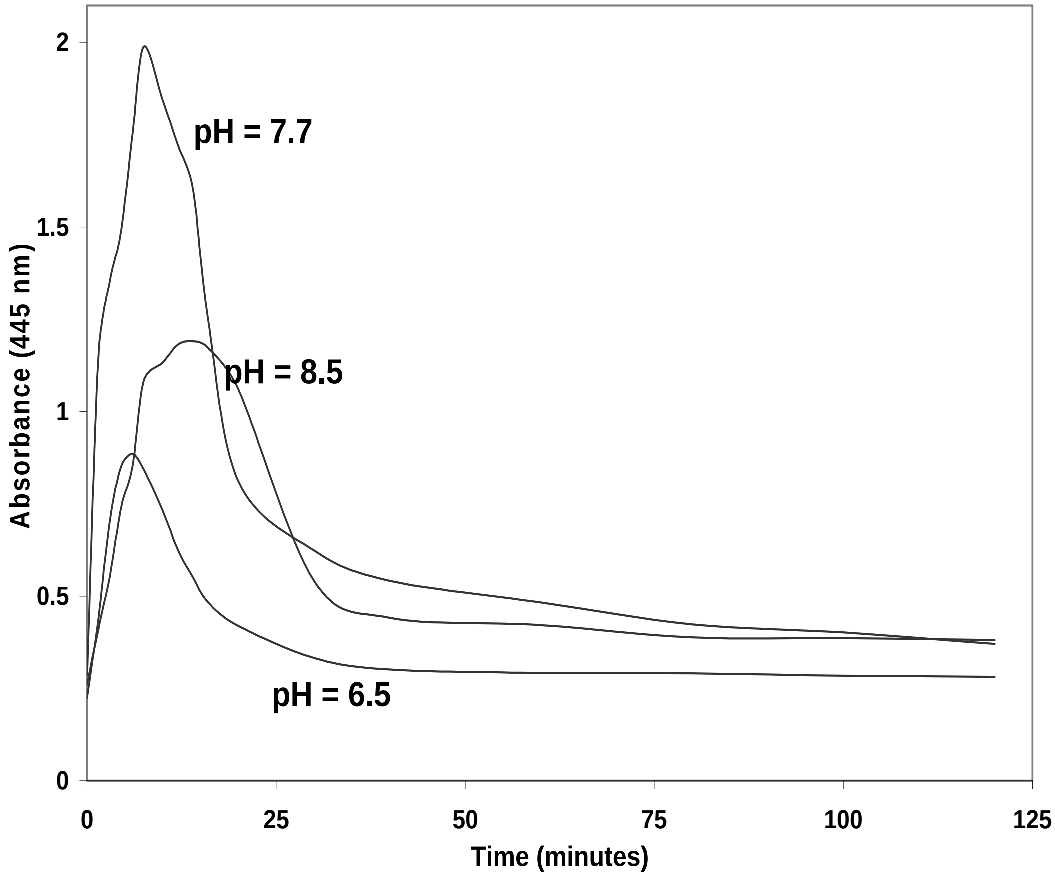

Figure 7**.** Investigating the Effect of pH on the Rate of Formation and Dissociation of the Intermediate at 445 nm

$[[CuSALAD]_2.H_2O]_0 = 0.00400$ M, $[H_2O_2]_0 = 0.00130$ M, $[2\text{-MeIm}]_0 = 0.0800$ M.

Table 4**.** *Initial Rates of Hydrogen Peroxide Decomposition vs. pH of Solution*

pH	Initial Rate (10^{-3} s^{-1})	R^2
6.5	2.667	0.9974
7.7	5.597	0.9891
8.5	1.627	0.9961

The pH studies indicated that a maximum rate of decomposition occurred when the overall pH of solution was closer to the pK_a of 2-methylimidazole.A plot of initial rate vs. pH dependence showed an initial increase in rate as pH increased up to about 7.7 followed by a decrease in rate as the pH was further increased (see Figure 8).

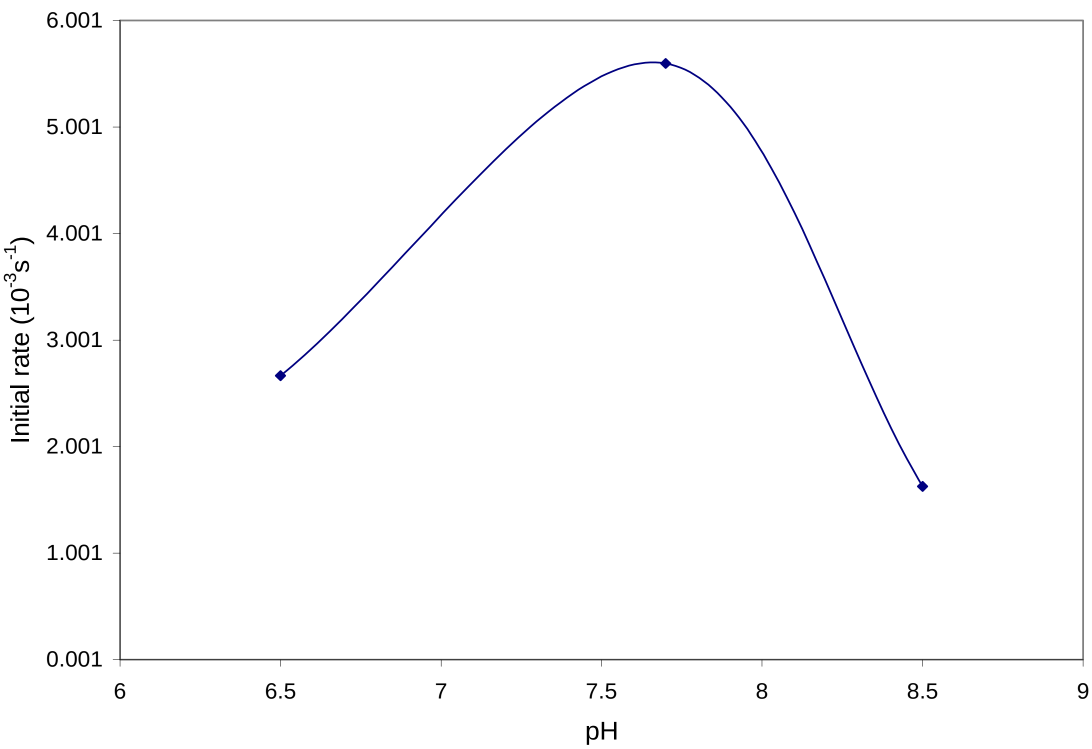

Figure 8. Initial Rate of Formation of the 445 nm Intermediate vs. pH of the Solution

The bell-shaped dependence of initial rate on pH suggested that there were two possible pre-equilibria preceding the decomposition of H_2O_2 by CuSALAD.B_2. The 2-MeIm was therefore thought to exist predominantly in the neutral form.

The dependence of the rate of formation of the intermediate at 445 nm in the absence of EDTA on the concentration of hydrogen peroxide was investigated and the results obtained are represented in Appendix C. The concentration of the catalyst was kept in excess of hydrogen peroxide. A plot of the results obtained is depicted in Figure 9. The results obtained for the dependence of the rate of formation of the 445nm intermediate on the concentration of the dimer ([CuSALAD]$_2$.H_2O]) are shown in Appendix D.

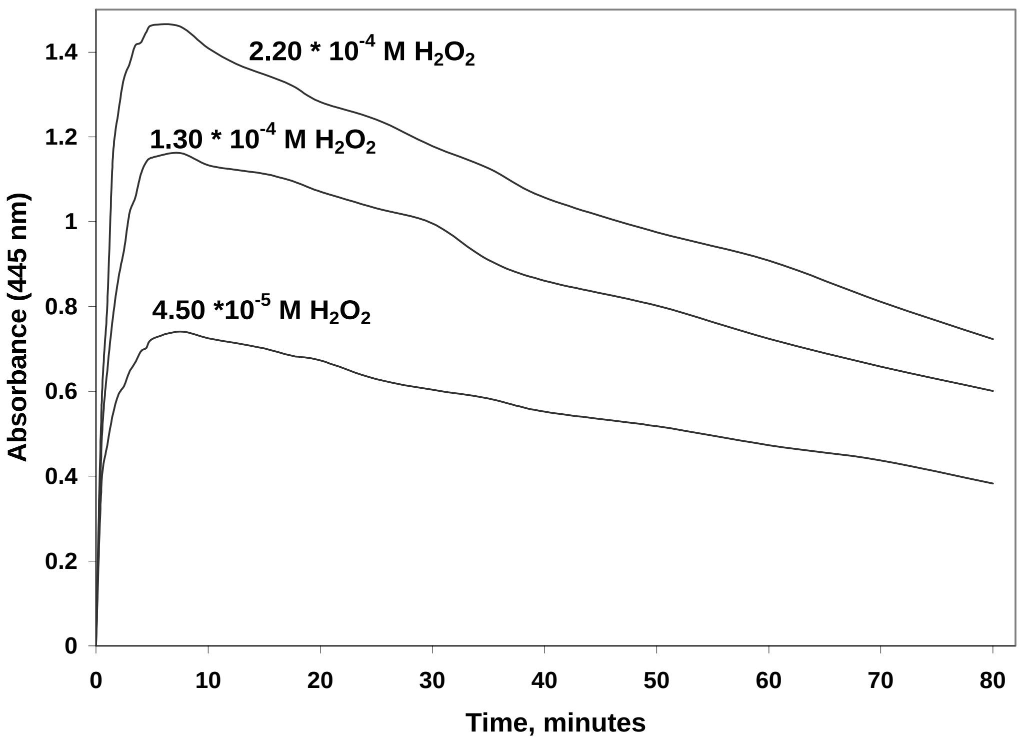

Figure 9. Progress Curves for the Variation of [H_2O_2] at constant [CuSALAD.B$_2$]

[CuSALAD.(2-MeIm)$_2$] = 0.00400 M.

The initial rate of formation of the 445 nm intermediate at constant concentration of hydrogen peroxide was investigated and the results are represented in Table 5.

Table 5. *Initial Rate vs.[[CuSALAD]$_2$.H_2O] with the Dimer in Excess of [H_2O_2], in the Absence of EDTA*

[[CuSALAD]$_2$], (10^{-4} M)	Initial rate, (10^{-2} s^{-1})	R^2
3.98	3.02	0.9993
7.96	5.00	0.9953
11.90	6.62	0.9977
23.90	11.46	0.9940

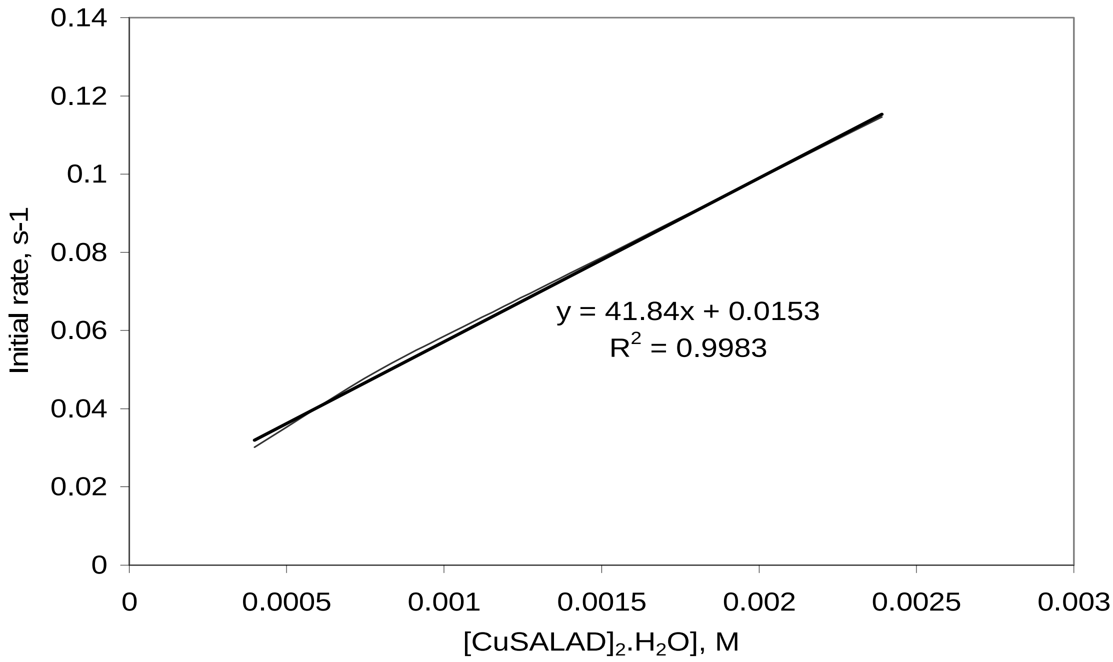

Figure 10. First-order Dependence of Initial Rate on [[CuSALAD]$_2$.H_2O] in Excess of [CuSALAD]$_2$, in the Absence of EDTA

[H_2O_2]$_0$ = 2.19 * 10^{-4} M, [2-MeIm]$_0$ = 4.00 * 10^{-2} M.

The initial rate of formation of the 445 nm intermediate in the hydrogen peroxide decomposition reaction at constant $[H_2O_2]_o$ (2.19 * 10^{-4} M), $[2\text{-MeIm}]_o$ (4.00 * 10^{-2} M), pH (7.7), temperature (25 ^oC) was studied as a function of the concentration of the $[CuSALAD]_2$ in the concentration range between 3.98 * 10^{-4} and 23.9 * 10^{-4} M. A graph of initial rate *vs.* the concentration of $[CuSALAD]_2$ yields a straight line conforming to the equation

$$\text{Initial rate} = k_1 + k_2 * [[CuSALAD]_2] = 1.5 * 10^{-2}\ s^{-1} + 41.8\ M^{-1}s^{-1} * [[CuSALAD]_2] \qquad (10)$$

The slope of the plot gives directly the value of k_2, which is a function of $[H_2O_2]_0$, and pH. The intercept, k_1 was considered to be significant relative to the k_2 term because the sum of the deviations of the values was less than the intercept. A significant k_1 value implied that some of the hydrogen peroxide decomposed appreciably through a catalyst-independent pathway. The non-zero interpretation of the intercept obtained from the plot of initial rate *vs.* concentration of catalyst led to the investigation of the effect of trace impurities of Cu(II) by using a catalyst-free copper(II) nitrate solution. Data representing the effect of trace copper(II) ions in the form of $Cu(NO_3)_2$ are found in Appendix G. Figure 11 shows a plot of the progress curves for the rate of decomposition of hydrogen peroxide by CuB_2 and by CuB_2 in the presence of $Cu(NO_3)_2$.

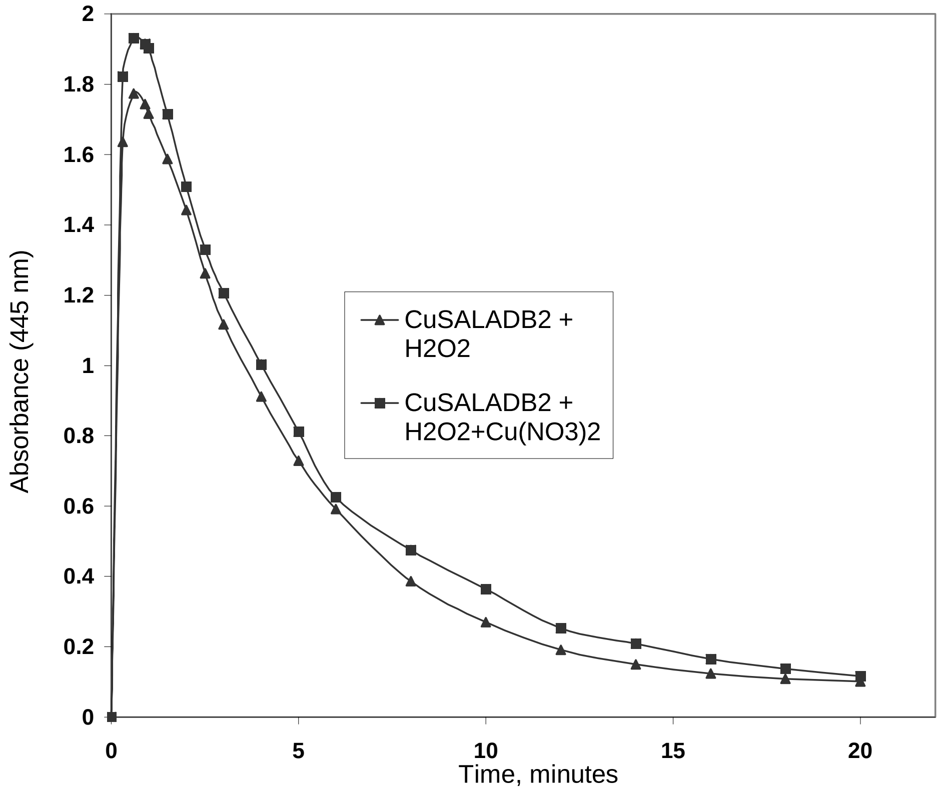

Figure 11. Studying the Effect of Cu(II) ion Impurities on the Rate of Decomposition of H_2O_2

A solution containing 0.10 mL of 0.00200 M $Cu(NO_3)_2$ and 1.0 mL of 0.00400 M CuSALAD.$(2\text{-MeIm})_2$ was used in this study. The concentration of hydrogen peroxide was constant (0.00440 M) in both kinetic runs. The rates were relatively faster in the case of the solution containing both the CuSALAD.B_2 and copper(II) nitrate than in the copper(II) nitrate-free solution. This result supported the thought that free Cu(II) ions or copper ions in the $[Cu(2\text{-MeIm})_2)]^{2+}$ form are capable of catalyzing the hydrogen peroxide decomposition reaction. However, kinetically speaking, the change was considered to be small and negligible because previous epr results [3] had not detected no free copper(II) ions in solution.

Data for the dependence of initial rate of formation of the intermediate at 445 nm on the catalyst concentration when hydrogen peroxide is in excess of the catalyst are represented in Table 6.

Table 6. *Initial Rates vs.[[CuSALAD]$_2$] with H_2O_2 in Excess of the Dimer, in the Absence of EDTA*

$[CuSALAD]_2]$, (10^{-4} M)	$[CuSALAD]_2]^2$, (10^{-8} M^2)	Initial rate, (10^{-2} s^{-1})	Fitted equation (k_1+k_2* $[Cu_2]^2$ (10^{-2})
1	1	0.38	0.39
2	4	1.09	1.10
3	9	2.35	2.28
4	16	3.91	3.93

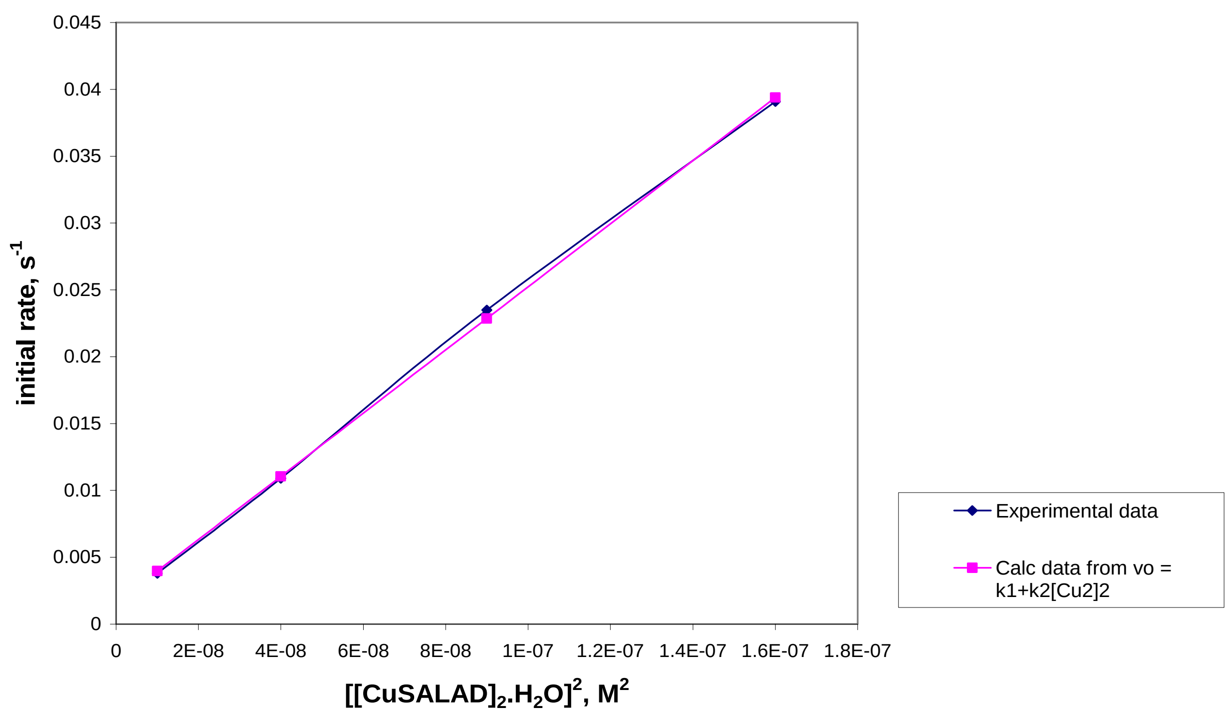

Figure 12. Initial Rates vs. [CuSALAD.B_2] in the Excess of H_2O_2 , in the Absence of EDTA

$[H_2O_2]_0 = 1.3 * 10^{-3}$ M, $[2\text{-MeIm}]_0 = 1.0 * 10^{-2}$ M. [CuSALAD.B_2] = 2* [[CuSALAD]$_2$] $k_1 = 1.60*10^{-3}$ s^{-1}, $k_2 = 2.36*10^5$ $M^{-2}s^{-1}$.

The plot of initial rate *vs.* $[[CuSALAD]_2]^2$ gave a straight line ($R^2 = 0.9992$) indicating a second-order rate dependence on $[CuSALAD.B_2]$. This suggested that the $CuSALAD.B_2$ species was involved in more than one elementary step of the hydrogen peroxide decomposition reaction or the initial rate method could be misleading in describing the overall picture. Therefore, in order to check that the information provided by the initial-rate method held up during the whole progress of the reaction, a kinetic run was performed for 60 minutes of the decomposition process.

Data representing the effect of variation of the concentration of hydrogen peroxide on the rate of formation of the intermediate at 445 nm when the catalyst is in excess of the hydrogen peroxide are shown in Table 7.

Table 7. *Initial Rates vs.*$[H_2O_2]$ *when* H_2O_2 *is in Excess of* $[CuSALAD]_2$*, in the Absence of EDTA*

$[H_2O_2]$, (10^{-4} M)	Initial rate, (10^{-2} s^{-1})
5.0	1.30
7.0	1.62
13	2.69
20	3.70
25	4.45

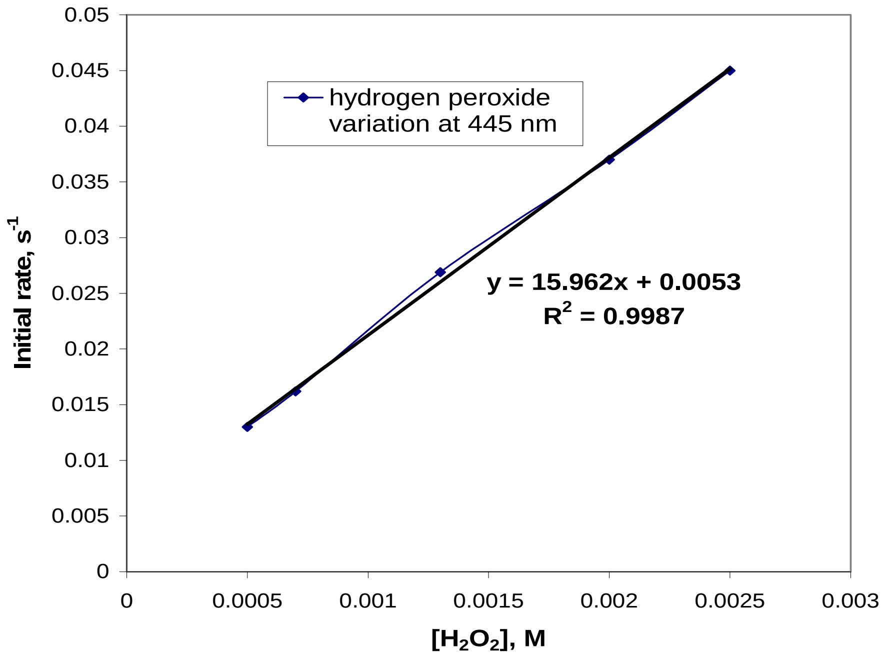

Figure 13. Initial Rates vs. $[H_2O_2]$ in the Absence of EDTA, in Excess H_2O_2

All rates were measured at an initial catalyst concentration of 1.00 * 10^{-4} M, pH of 7.7, $[2\text{-MeIm}]_0$ = 1.00 * 10^{-2} M, 60/40 EtOH/H_2O solvent, $k_1 = 5.3*10^{-3}\ s^{-1}$, $k_2 = 15.96\ M^{-1}s^{-1}$. The intercept of the plot, k_1, is zero within experimental error.

The dependence of the initial rate of formation of the intermediate at 445 nm on the concentration of hydrogen peroxide when the hydrogen peroxide is in excess of the catalyst was determined and data obtained were represented in Table 8. The reaction was carried out in the absence of EDTA. Figure 14 shows a plot of the results obtained from initial rate studies.

Table 8. *Initial Rates vs.[H_2O_2] when the Dimer is in Excess of H_2O_2, in the Absence of EDTA*

[H_2O_2], (10^{-4} M)	Initial rate, (10^{-3} s^{-1})	R^2
2.75	3.1	0.9993
4.00	5.5	0.9958
6.00	9.6	0.9988
8.00	13.1	0.9996

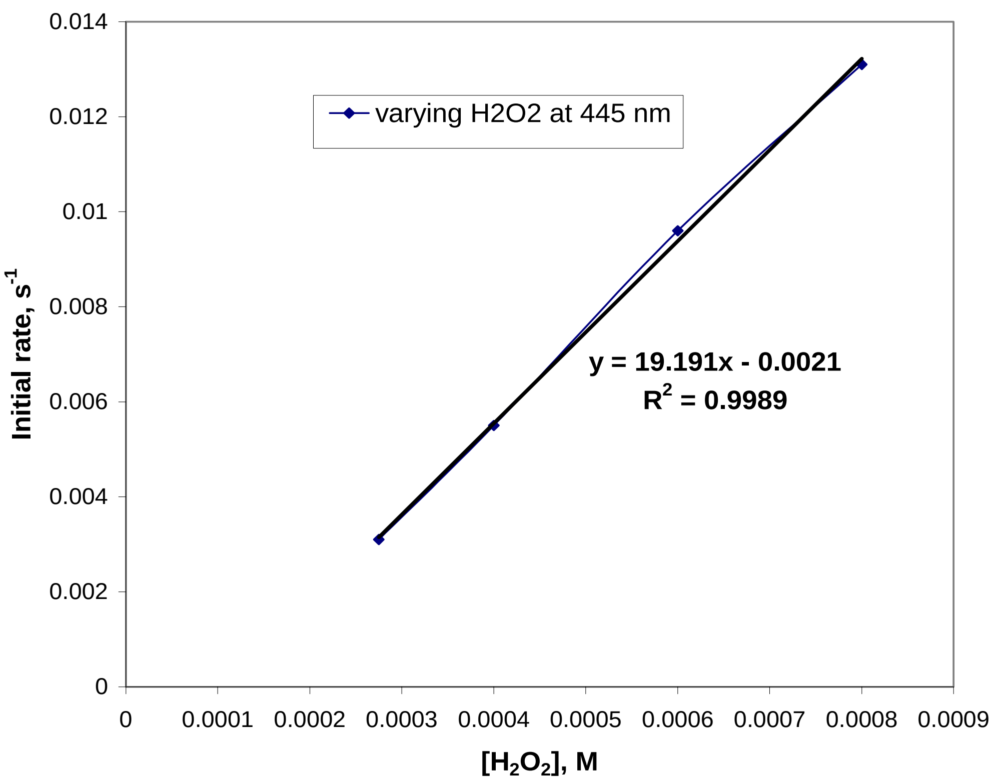

Figure 14. Initial Rates vs. [H_2O_2] in the Absence of EDTA, in Excess [CuB_2]

[2-MeIm]$_0$ = 8.0*10^{-2} M, [[CuSALAD]$_2$]$_0$ = 4.0*10^{-3} M, 70/30 EtOH/H_2O solvent

A plot of Initial rate *vs.* [H_2O_2] gave a straight line with a slope of 19.2 $M^{-1}s^{-1}$. The intercept is zero within experimental error. The slope (19.2 $M^{-1}s^{-1}$) is approximately equal to the slope obtained when hydrogen peroxide is in excess of the CuB_2 adduct (15.96 $M^{-1}s^{-1}$).

The effect of EDTA on the initial rate of formation of the 445 nm intermediate was investigated and the results showed in decrease in both the intensity of the CT band and the rate of decomposition of hydrogen peroxide. Data representing the dependence of initial rates on the catalyst concentration are shown in Table 9. A plot of the data is shown in Figure 15.

Table 9. *Initial Rates vs. [CuSALAD.B_2] in the Presence of EDTA*

[[CuSALAD]$_2$], (10^{-4} M)	[CuSALADB_2], (10^{-4} M)	Initial rate, (10^{-3} s^{-1})	R^2
4.0	8.0	0.5	0.9988
7.3	14.3	1.3	0.9965
9.9	19.8	1.8	0.9946
16	32	3.4	0.9955

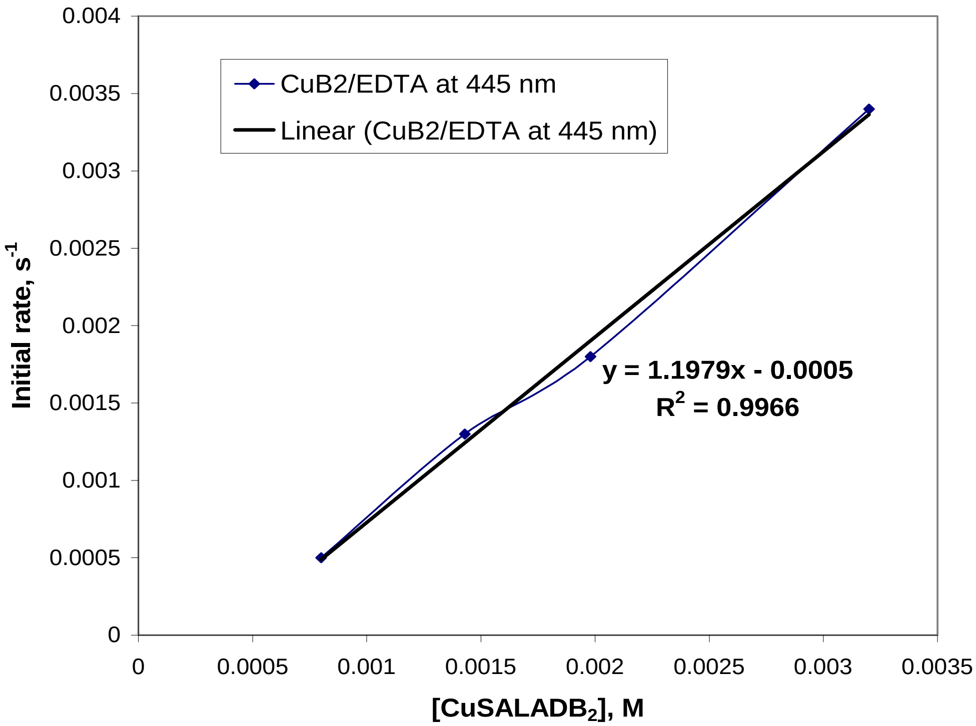

Figure 15. Initial Rates vs. [CuSALAD.B_2] in the Presence of EDTA

[CuSALAD.B_2] = 2* [[CuSALAD]$_2$],[2-MeIm]$_0$ = $4.00*10^{-2}$ M, [H_2O_2]$_0$ = $2.19*10^{-4}$ M

The plot of Initial rate *vs.* [CuSALAD.B_2] gave a straight line with a slope of 1.198 $M^{-1}s^{-1}$, suggesting a first-order dependence of rate on the concentration of catalyst. The intercept is zero within experimental error. The EDTA appears not only to behave as a sequestering agent for Cu(II) or $[Cu(2\text{-}MeIm)_2]^{2+}$ but also scavenges the hydroxyl radical if any was formed during the decomposition reaction. However, a separate experiment using another hydroxyl radical scavenger, methanol, was performed to ascertain the absence of hydroxyl radicals in the reaction medium. Therefore, the possible role of EDTA was limited to the complexation of any Cu(II) ions that were present in solution either freely or in the form of the $[Cu(2\text{-}MeIm)_2]^{2+}$ complex, thereby slowing down the rate of hydrogen peroxide decomposition. The EDTA could possibly be reacting with any Cu(II)-hydroxy species present in solution. Previous studies [5] had reported the stability of the Cu(II)-hydroxy species around the 400 – 450 nm region.

The dependence of initial rates on the concentration of hydrogen peroxide in the presence of EDTA was investigated and the results were represented in Table 10. The plot of the results is obtained and represented in Figure 16.

Table 10. *Initial Rates vs. [H_2O_2] in the Presence of EDTA*

[H_2O_2], 10^{-3} M	Initial rate, 10^{-4} M
0.6	4.3
1.9	20.1
3.0	32.5
6.5	71.0

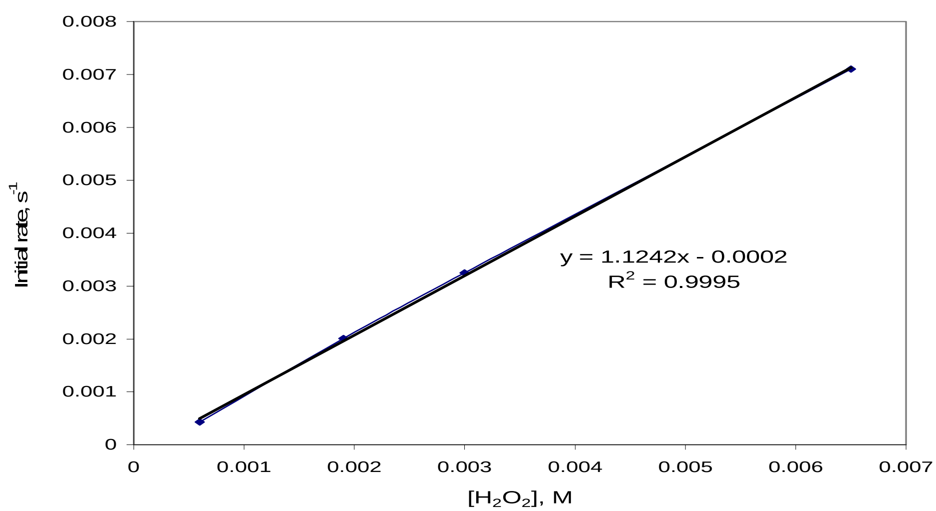

Figure 16. Initial Rates vs. [H_2O_2] in the Presence of EDTA

[[CuSALAD]$_2$.H_2O]$_0$ = 0.00400 M, [2-MeIm]$_0$ = 0.0800 M.

A Plot of initial rate *vs.* [H_2O_2] gave a straight line with a slope (k_2 term) of 1.124 $M^{-1}s^{-1}$. The intercept is zero within experimental error. The correlation coefficient, R^2 was 0.9995. The straight line indicated a first-order dependence of the initial rate of formation of the 445 nm CT intermediate peak on [H_2O_2] in the presence of EDTA. Table 11 summarizes the results showing all the relative rate coefficients and goodness parameters obtained from the method of initial rates.

Table 11. *Relative Rate Coefficients and Goodness Parameters Obtained from Initial Rate Studies*

	Varying [CuB_2], xs CuB_2, no EDTA	Varying [CuB_2], xs H_2O_2, no EDTA	Varying [CuB_2] in EDTA	Varying [H_2O_2], xs H_2O_2, no EDTA	Varying [H_2O_2], xs CuB_2, no EDTA	Varying [H_2O_2] in EDTA
Slope, k_2, $M^{-1}s^{-1}$	83.68	$2.36 * 10^5$	1.20	15.96	19.19	1.12
Intercept, k_1, s^{-1}	$1.53 * 10^{-2}$	$1.60 * 10^{-3}$	~0	~0	~0	~0
Specific order	1	2	1	1	1	1
R^2	0.9983	0.9992	0.9966	0.9987	0.9989	0.9995

The overall rate of formation and decay of the 445 nm intermediate was equally investigated both in the absence and presence of EDTA in an attempt to understand the entire reaction profile and propose mechanistic steps that were consistent with the results obtained from initial rate studies. The rate studies for the overall decomposition process also helped to explain any discrepancies in the results obtained by methods of initial rates. Data representing the results obtained from the Isolation method (see Experimental section) for both the hydrogen peroxide decomposition reaction in the presence and absence of EDTA are shown in Appendix E. The calculated values for the concentration of the 445 nm intermediate were plotted on the same scale as the experimental values of the intermediate in the absence of EDTA (Figure 17), and in the presence of EDTA (Figure 18).

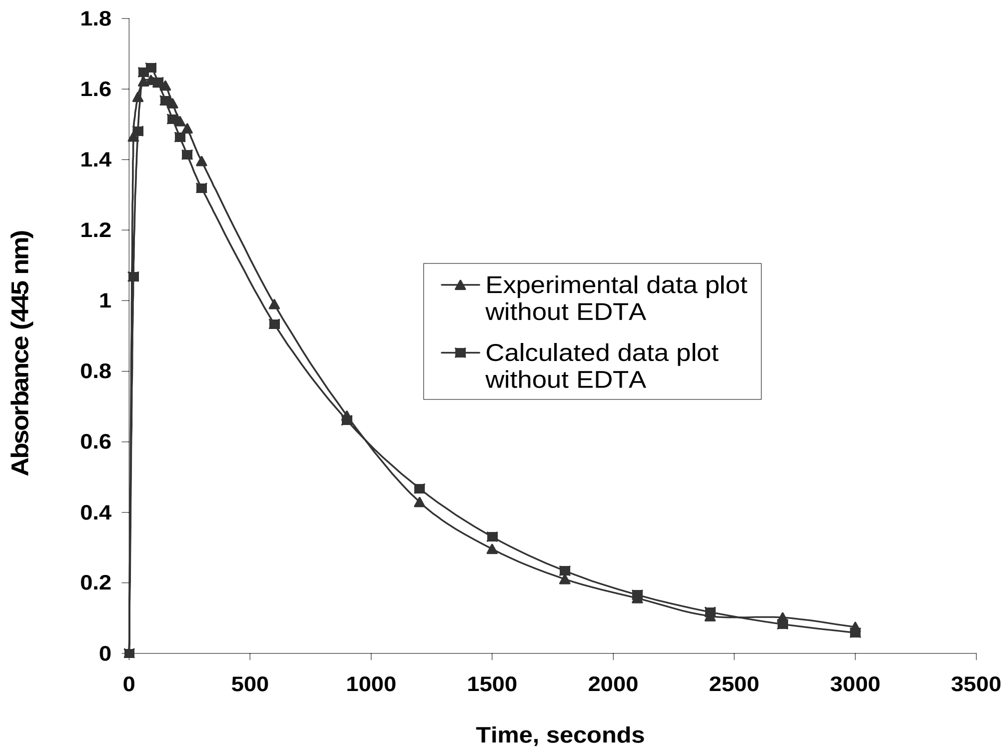

Figure 17. Comparison of Experimental and Calculated Plots in the Absence of EDTA

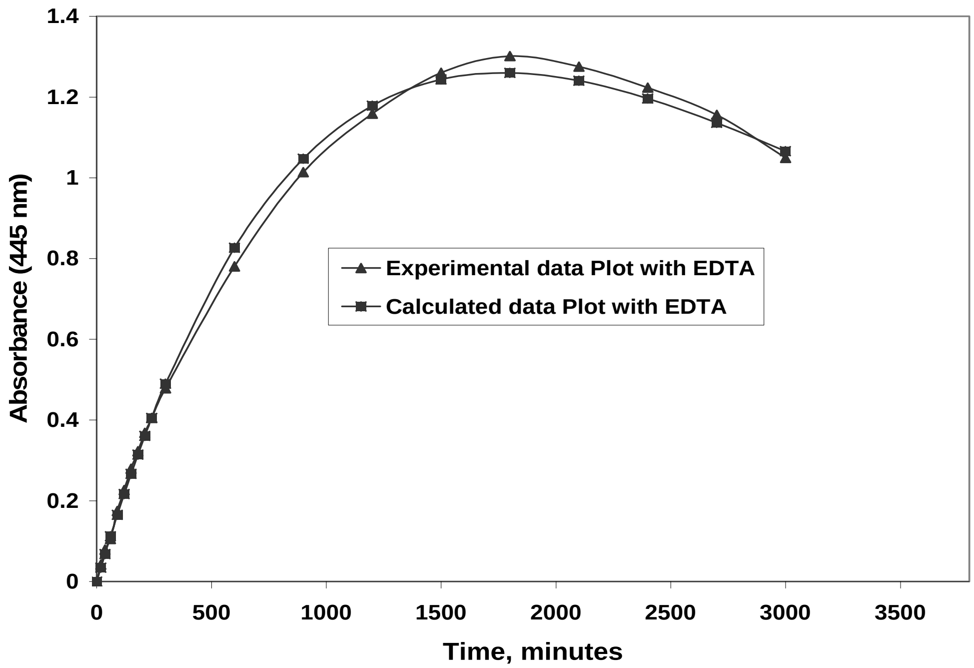

Figure 18. Comparison of Experimental and Calculated Plots in the Presence of EDTA

The rate of reaction slowed down considerably in the presence of EDTA suggesting that EDTA participated in the reaction by possibly tying up one of the species that was thought to increase the rate of decomposition of hydrogen peroxide. The figures also show how the calculated plots compare with experimental plots thus providing an insight to the type of mechanism because the data were fitted based on a proposed mechanism. The concentration of hydrogen peroxide was kept in a 10- or higher-fold excess over that of the catalyst, CuB_2 so that rate changes were approximated to be due to changes in the concentration of $[CuSALAD]_2$. $k_{obsd} = k[H_2O_2]_0$. k can be obtained by varying the concentration of hydrogen peroxide and making a plot of k_{obsd} *vs.* $[H_2O_2]$. The slope of the plot gives the value of k.

The following reaction scheme as previously indicated in the experimental section was then used. to fit the experimental data;

$$A \longleftrightarrow B \qquad k_f, k_r$$

$$B \longrightarrow C \qquad k_d$$

$$[B] = \frac{k_f [A]_0 \{\exp(-k_f t) - \exp(-(k_r + k_d)t\}}{k_d + k_r - k_f}$$

k_f = forward rate constant, k_r = reverse rate constant, k_d = dissociation constant, $[A]_0$ = initial concentration of $[CuSALAD]_2.H_2O$. [B] represents the concentration of intermediate (formed at 445 nm) at time, t. C represents the product(s) of the reaction or simply the short-lived species that once formed, immediately decompose(s) to form the products. Using this equation, guess values for the different parameters were chosen and then adjusted to obtain the best possible fit between the experimental and calculated values. Scientist and MathCAD were used for obtaining approximate values for the relative rate coefficients and Excel 2003 was then used to treat all the data because it was easily affordable. The calculated results for the EDTA-free solution and EDTA-containing solution are represented in Table 11.

Table 12. *Rate Parameters Obtained from Curve Fitting in the Absence and Presence of EDTA*

$[2\text{-MeIm}]_0$ = 0.0800 M, $[H_2O_2]_0$ = 0.00440 M, $[[CuSALAD]_2.H_2O]_0$ = 0.000200 M

Solution content	k_f (forward rate constant) in s^{-1}	k_r (reverse rate constant) in $M^{-1}s^{-1}$	k_d (dissociation rate constant) in s^{-1}	Standard deviation, s	Correlation Coefficient, R^2
$CuSALADB_2 + H_2O_2$	0.0500	0.000500	0.000650	0.1036	0.9796
$CuSALADB_2$ + EDTA + H_2O_2	0.000566	0.00000626	0.000560	0.0251	0.9976

Data depicting the effect of methanol, a free radical scavenger on the rate of formation and decay of the 445 nm intermediate are represented in Appendix H and a plot of the data is shown below (Figure 19).

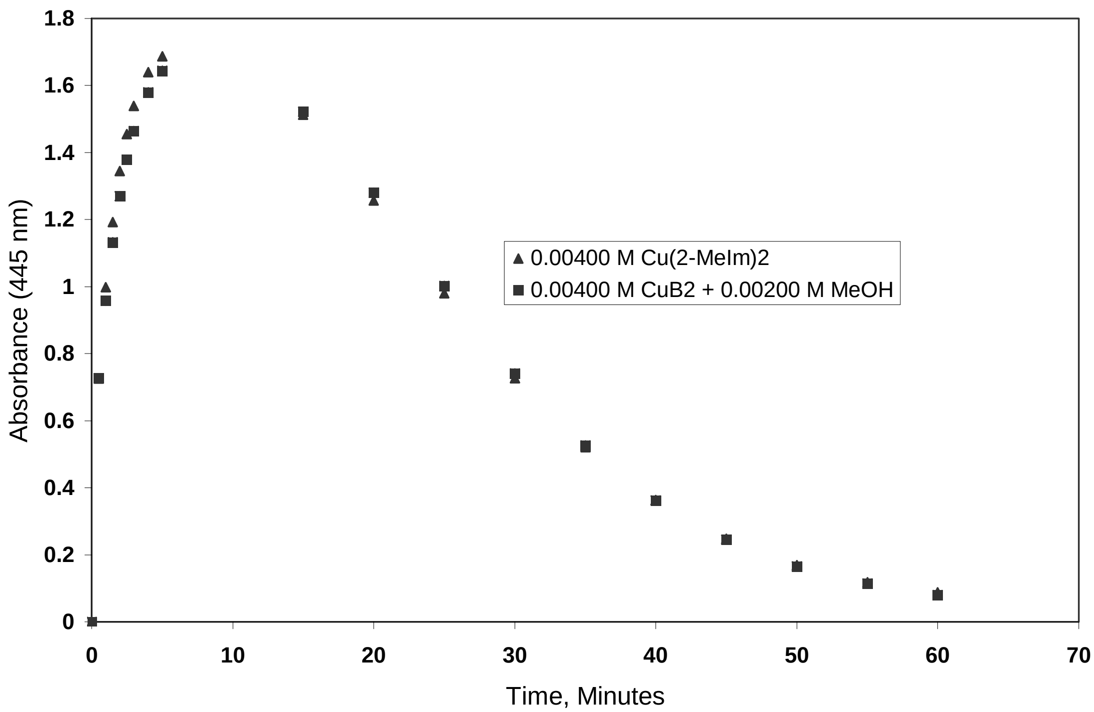

Figure 19. Rates of Decomposition of H_2O_2 in the Absence and Presence of MeOH

$[Cu(2\text{-}MeIm)_2]_0$ = 0.00400 M, $[MeOH]_0$ = 0.00200 M.

The plots of the methanol-free and MeOH-containing solutions were almost identical in shape. This showed that methanol had no effect on the rate of decomposition of hydrogen peroxide hence there were no hydroxyl radicals in the reaction medium.

CHAPTER 4
DISCUSSION

Determination of Molecular Weight of $[CuSALAD]_2$

Freezing point depression and vapor pressure lowering experiments were used to confirm the dimeric nature of the Cu(II) complex that had been previously reported [3]. The calculated value for the molecular weight of the dimeric form of $[CuSALAD]_2.H_2O$ from atomic weight data is 683 g/mol. When a solution of $[CuSALAD]_2$ and benzene, or ethanol is agitated until equilibrium is attained and the solutions made dilute enough, ideal behavior is assumed. Solutions or mixtures are considered to be ideal when all the components in the mixture or solution have matched intermolecular forces. The concordance of literature (5.120 ^{o}C/mol, for T_f = 5.530 ^{o}C), [14] and experimental (5.072 ^{o}C/mol for T_f =5.545 ^{o}C/mol, see Table 1) values for the molal freezing-point depression constants is greater in the case of dilute solutions. The values obtained from an average of three trials using freezing point depression (in benzene solvent) and vapor pressure lowering (in ethanol solvent) measurements are 731 and 700 g/mol respectively (see Tables 1 and 2 respectively). From the fact that the experimental values agree closely with the calculated value for the dimeric structure of the copper(II) complex (683 g/mol) than with the monomeric structure, $CuSALAD.H_2O$ (M. W. = 350.5 g/mol), we conclude here that the copper(II) complex is dimeric in nature. These results confirm previous results [3] and give better agreement than previously reported data.

Determination of $[CuSALAD]_2.H_2O$: 2-MeIm Stoichiometric Ratio

It has been previously shown that $[CuSALAD]_2$ reacts with different bases to establish an equilibrium in ethanol or aqueous ethanol solutions. Previous experiments in our laboratory in which the intensities of the epr signals of the CuB_2 adducts were monitored [3], showed a 4:1 ratio of imidazole, 1-MeIm and L+AD to $[CuSALAD]_2.H_2O$. There are two possible equilibria that are involved in the reaction of 2-MeIm (an organic base) with the dimer in ethanol or aqueous ethanol solvents. The $[CuSALAD]_2.H_2O$ complex will henceforth be abbreviated as Cu_2, and the $CuSALAD.B_2$ adduct as CuB_2.

$$Cu_2 + 2B \Longleftrightarrow 2CuB \qquad (11)$$

$$2CuB + 2B \Longleftrightarrow CuB_2 \qquad (12)$$

The absorbance spectrum (Figure 2) of the Cu(II)-B adduct is consistent with a tetragonal square pyramidal structure for the $CuSALAD.B_2$ adduct with a $(d_{x2-y2})^1$ ground state. As incremental portions of the base, 2-MeIm, are added to an aqueous ethanol solution of $[CuSALAD]_2.H_2O$, the absorbance maximum shifts to lower wavelengths with an increase in intensity as the two equilibria represented above are shifted toward the formation of the $CuSALAD.B_2$ adduct. The definite break (at 595 nm) at a 4 : 1 stoichiometric ratio of 2-MeIm to dimer is consistent with the results of the epr studies carried out on the other bases in our laboratory.

Preliminary Qualitative Test Results

Previous kinetic studies involving the $[CuSALAD]_2$-ImH and hydrogen peroxide suggested that the progress of the reaction could be monitored through spectroscopic methods by tracking the spectrally active species that absorbed around the 450 nm region. The most recent studies equally indicated that the maximum rate of decomposition of hydrogen peroxide was directly proportional to the pH or pKa of the imidazole or methyl substituted imidazole under consideration [5]. Our studies suggest that 2-MeIm is the most reactive imidazole derivative (see Tables 3 and 4) and its pKa value (7.77) lies between that if ImH (6.90) and 4-MeIm (8.35). Each imidazole derivative shows faster rates when the pH of the buffered system is at or near the pKa of the imidazole under consideration (see Table 4, Figures 7 and 8).

A study of the decomposition of H_2O_2 by Cu^{II}-Im complexes showed that the hydrogen peroxide decomposition reaction could be catalyzed by $Cu(Im)_2^{2+}$, the catalytically active species [6]. Another possible role of the imidazole or methyl substituted imidazole in the $CuSALADB_2$ form is their ability to stabilize the copper in the +2 oxidation state. By maintaining a very high excess of [B] over $[CuSALAD]_2$, the dimeric complex is completely converted into the $CuSALADB_2$ adduct (see equations 11 and 12), which is the catalyst in the hydrogen peroxide decomposition reaction.

The facts that 2-MeIm gives the fastest initial rates (see Table 3) with greater spectral intensities, in comparison with ImH and 4-MeIm make it the base of choice in this study.

The (initial) rates vary with pH of the solutions (Table 4) with 2-MeIm being used as the base of choice. Maximum changes occur near the pKa of 2-MeIm (see Figure 8). While the rate is slow at low pH (pH 6.5), it increases as pH increases (pH 7.7), and finally decreases as the pH is further increased (pH 8.5). The bell-shaped plot shown in Figure 8 suggests that there are two possible equilibria preceding the rate determining step of the reactions involved in the catalytic decomposition of hydrogen peroxide. These pre-equilibria are represented in the following equations:

$$BH_2^+ \longleftrightarrow BH \longleftrightarrow B^- \qquad (13)$$

The base therefore exists predominantly in the neutral form because pH results indicate a maximum in initial rates at a neutral pH range.

The observation that the initial rates appeared to slow down noticeably when an aqueous ethanol solvent was used as opposed to using only ethanol indicates that water plays a role in the reaction. This suggests that there is a competitive reaction between H_2O_2 and H_2O, for a vacant coordination site on the copper catalyst.

There are at present many different tenable models for the mechanism of the decomposition of hydrogen peroxide in the presence of different inorganic catalysts. Our experimental results will now be discussed in terms of two different mechanisms.

Reaction Mechanism in the Absence of EDTA

The following mechanistic steps can be envisioned for the pathway predominant at low catalyst concentrations in the absence of EDTA:

$$CuB_2 + H_2O_2 \longleftrightarrow CuBOOH^+ + BH^+ \qquad (14)$$

$$CuBOOH^+ + CuB_2 \longrightarrow CuBOOCuB + BH^+ \qquad (15a)$$

$$CuBOOH^+ + Cu^*(II) \longrightarrow CuBOOCu^* + H^+ \qquad (15b)$$

$$CuBOOCuB + BH^+ \longrightarrow CuBOH^+ + CuB_2 + 1/2O_2 \qquad (16a)$$

$$CuBOOCu^* + BH^+ + H^+ \longrightarrow CuB_2 + 1/2O_2 + H_2O + Cu^* \qquad (16b)$$

$$CuBOH^+ + BH^+ \longrightarrow CuB_2 + H_2O \qquad (17a)$$

Two possible mechanisms can be proposed based on the results obtained from the kinetic studies. Equations (14), (15a), (16a), and (17a) give rise to the initially suggested pathway characterized by the second-order dependence of initial rates of formation of the 445 nm intermediate on the concentration of the catalyst. Equations (14), (15b), and (16b) form the other mechanistic pathway characterized by the first-order dependence of initial rates on the concentration of the catalyst. The overall reaction in both cases is

$$H_2O_2\ (aq) \longrightarrow H_2O\ (l) \quad + \quad 1/2O_2\ (g) \qquad (18)$$

Cu*(II) is used to represent the form of the copper impurity detected in solution either as free copper(II) ions or as $[Cu(2\text{-MeIm})_2]^{2+}$. In the first step, Eq. (14), complexation of CuB_2 by H_2O_2 leads to the formation of the mononuclear hydroperoxo ($CuBOOH^+$) intermediate. Some evidence in support of this intermediate comes from the charge transfer (CT) band observed around the 450 nm region (445 nm for 2-MeIm, see Figure 3).

In the presence of more H_2O_2 over CuB_2, initial rate studies point to a second-order dependence of rate on the concentration of CuB_2 (see Table 6, Figure 12) and a first-order dependence on the concentration of H_2O_2 (see Table 7, Figure 13) with slopes, $2.36 * 10^5\ M^{-1}s^{-1}$ and $15.96\ M^{-1}s^{-1}$ respectively. The intercepts are respectively $1.60 * 10^{-3}s^{-1}$, corresponding to the catalyst-independent pathway, and zero (within experimental error). Spectral evidence collected during the preliminary qualitative tests point to the existence of a second intermediate (Figure 3) around the 420 nm region (418 nm for 2-MeIm). This intermediate was identified as being of the binuclear category; peroxo 'end-on' Cu_2O_2. The peroxo, 'side-on' Cu_2O_2 structure is expected to show an intense peak around 300-400 nm. No absorption signal was observed around this region pointing to the absence of the 'side-on' Cu_2O_2.

Even after it was understood that the peroxo, 'end-on' Cu_2O_2, was responsible for the CT band around 420 nm, there was some ambiguity as to whether it was CuBOOCuB, formed from the interaction of CuB_2 with the first intermediate, $CuBOOH^+$ in Eq. (15a),or it was CuBOOCu*, formed from the reaction of $CuBOOH^+$ with free Cu(II) ions in solution in Eq (15b) or copper(II) ions complexed with the 2-MeIm in the form $[Cu(B)_2]^{2+}$. However, when more CuB_2 than H_2O_2 is present in solution, the reaction is first-order in CuB_2 and reaction (15b) appears to predominate. The peroxo 'end-on' Cu_2O_2 may be assigned the structure CuBOOCuB, in the presence of more H_2O_2, if the second-order dependence of initial rates on CuB_2 is considered to be significant and CuBOOCu*, if the impurity effect is more significant. However, because EDTA didn't destroy the CuB_2 complex, reaction (15a) should still have occurred in the presence of EDTA but the 420 nm intermediate was only slightly stable in the presence of EDTA. Hence, the second intermediate is assigned to CuBOOCu* and reaction (15b) predominates.

The rate of reaction is first-order in H_2O_2, and is independent of whether or not hydrogen peroxide is in excess of CuB_2. This suggests that H_2O_2 is involved in only one of the envisioned mechanistic steps of the proposed mechanisms, thereby providing evidence why the previously assigned intermediate of the form $Cu(OOH)_2$ [9-13], formed by the reaction

$$CuBOOH^+ \quad + \quad H_2O_2 \longleftrightarrow Cu(OOH)_2 \quad + \quad BH^+ \qquad (19)$$

was not observed and hence was not assigned. Further evidence to support this thought comes from the fact that a plot of approximate dissociation rate coefficients (obtained from Figure 9) *vs.* $[H_2O_2]$ point to a zero-order dependence on H_2O_2.

Even though independent rate studies with respect to the base, [B], have not been reported, it was observed that rates increased with an increase in B up to a maximum and began to decrease. The initial increase was due to the formation of CuB_2, catalyzing the hydrogen peroxide decomposition reaction. As the catalyst is complexed with H_2O_2, a molecule of base is released. The downward turn in the reaction rate in the presence of excess 2-MeIm is attributed to the increasing competition between the 2-MeIm and peroxide for the coordination site on the $[CuSALAD]_2$ complex. The following equations show the competitive process;

$$[CuSALAD]_2 + 4\,B \longleftrightarrow 2\,CuSALAD.B_2 \tag{20}$$

$$CuSALAD.B_2 + H_2O_2 \longleftrightarrow CuSALAD.B(OOH) + BH^+ \tag{21}$$

$$BH^+ \longleftrightarrow H^+ + B \longleftrightarrow B^- + H^+ \tag{22}$$

The trend of increase then decrease in initial rate as the concentration of the base, 2-MeIm is varied appears to parallel the trend in pH. Table 4 shows how the rate doubles with and increase in pH (from 6.5 to 7.7) and then drops about 3 times as the pH is further increased to 8.5. The bell-shaped plot obtained from these results is shown in figure 8. It suggests that there are two possible pre-equilibria preceding the catalytic decomposition of hydrogen peroxide by CuSALAD.$(2\text{-MeIm})_2$. The base, 2-MeIm is therefore thought to exist predominantly in the neutral form since the highest rates were obtained around neutral pH region, 7.7, (see equation 22).

Reaction Mechanism in the Presence of EDTA

The rate of formation of the intermediate at 445 nm appeared to slow down tremendously in the presence of EDTA and the stability of the 420 nm CT band decrease considerably after the first 5 minutes of the reaction. For such a pathway that is predominant at intermediate values of catalyst concentration, in the presence of EDTA, the following mechanistic steps have been proposed:

$$CuB_2 + H_2O_2 \longleftrightarrow CuBOOH^+ + BH^+ \qquad k_f, k_r \tag{14}$$

$$CuBOOH^+ \longrightarrow CuBOH^+ + 1/2O_2 \qquad k_d \tag{23}$$

$$CuBOH^+ + BH^+ \longrightarrow CuB_2 + H_2O \tag{24}$$

Using the Isolation (Flooding) method by making $[H_2O_2] >> [CuB_2]$ so that $[H_2O_2]$ is effectively constant during the course of the reaction,

$$k_{obsd} = k\,[H_2O_2] \tag{25}$$

but $[CuB_2] = [CuB_2]_0 - [CuBOOH^+]$, (because all of the intermediate comes from the catalyst). Omitting $[BH^+]$ (the concentration of base is in such a large excess that it remains fairly constant) in the treatment that follows, we can solve for $[CuBOOH^+]$.

$$d\,[CuBOOH^+]/dt = k_f\,[CuB_2] - k_r\,[CuBOOH^+] - k_d\,[CuBOOH^+] \tag{26}$$

Because the catalyst decays via a first order pathway, $[CuB_2]$ becomes

$$[CuB_2] = [CuB_2]_0 * \exp(-k_f t) \tag{27}$$

where $[CuB_2]_0$ is the initial concentration of the catalyst. Substituting the right hand side of equation (27) for $[CuB_2]$ in equation (26) and grouping like terms together gives

$$d\,[CuBOOH^+]/dt = k_f\,[CuB_2]_0 \exp(-k_f.t) - (k_r + k_d)\,[CuBOOH^+] \tag{28}$$

Solving equation (28) for $[CuBOOH^+]$ gives

$$[CuBOOH^{+}] = \frac{k_f [CuB_2]_0 \times \{\exp(-k_f t) - \exp(-(k_r + k_d)t)\}}{k_d + k_r - k_f} \tag{29}$$

$$\text{rate} = k_d [CuBOOH^{+}] = \frac{k_d k_f [CuB_2]_0 \times \{\exp(-k_f t) - \exp(-(k_r + k_d)t)\}}{k_d + k_r - k_f} \tag{30}$$

Equation (29) was used to fit the experimental data in an attempt to elucidate the reaction mechanism and obtain the different relative rate coefficients (see Table 12 and Figures 17 and 18) in the absence and presence of EDTA. The first step of the mechanism is identical in form to that of the above mechanism that has been proposed in the absence of EDTA. Upon injection of EDTA into the reaction mixture, spectral evidence collected during the scoping tests point to the stability of the 445 nm intermediate after the first 5 minutes (see Figure 5), and the rate slows down about 100 times (Figure 18, table 12).

EDTA is a strong complexing/sequestering ligand that appears to complex Cu*(II) ions in solution leading to the decrease in stability of the CuBOOCu* intermediate that was initially observed around the 420 nm region and thus assigned in the first reaction pathway. The measure of the binding ability (pK) of $Cu(EDTA)^{2-}$ at a temperature of 20 ^{o}C and an ionic strength of 0.10 is reported to be 18.86 [21

$$Cu^{2+} + EDTA \longleftrightarrow Cu(EDTA)^{2-} \tag{31}$$

$$[Cu(2\text{-}MeIm)_2]^{2+} + EDTA \longleftrightarrow Cu(EDTA)^{2-} + 2\,(2\text{-}MeIm) \tag{32}$$

Because the concentration of the base was kept in large excess, the most likely structure for the Cu(II)-base impurity complex is $Cu(2\text{-}MeIm)_4^{2+}$ but the catalytically active species has been shown in previous studies [6] to be $Cu(Im)_2^{2+}$. During the complexation process, it is thought that the EDTA does not destroy the $CuSALAD.B_2$ complex. This is supported by the fact that there is no visible color change from the bluish-purple color of CuB_2 when the ratio of the concentration of EDTA to that of CuB_2 is approximately equal to one and the solutions are mixed thoroughly. Another piece of evidence comes from the observation that the peak position and intensity of the 595 nm d-d absorption band of the CuB_2/EDTA system (Figure 4) is almost identical to that of the EDTA-free solution with only a 6% decrease that is attributed to dilution. Therefore, the reaction possibilities shown below are not thought to be occurring.

$$CuSALAD.B_2 + EDTA \longleftrightarrow CuEDTA + SALAD + 2B \quad (33)$$

$$CuSALAD.B_2 + EDTA \longleftrightarrow CuSALAD.EDTA + SALAD + 2B \quad (34)$$

Initial rate studies indicate that the rate is first-order in CuB_2 and first-order in H_2O_2 (Table 11). The intercept of figure 15 is set to zero which physically means that no catalyst-independent decomposition of hydrogen peroxide occurs in the presence of EDTA. Comparing this zero value to that in the absence of EDTA ($1.5 *10^{-2}\ s^{-1}$, Table 11), we see that EDTA complexes all of the Cu*(II) species in solution that is responsible for the non zero intercept and also for the decrease in rates in the presence of EDTA. From Table 12, we see that the formation constant, k_f is approximately 100 times greater than both the reverse rate constant, k_r and the dissociation constants, k_d, in the absence of EDTA. However, in the presence of EDTA, k_f and k_d are about the same ($k_f = 5.66 * 10^{-4}\ s^{-1}$ and $k_d = 5.60 * 10^{-4}\ s^{-1}$) whereas k_r is approximately 100 times lower ($k_r = 6.26 * 10\text{-}6\ M^{-1}s^{-1}$). Previous epr studies [3] done on the $[CuSALAD]_2.H_2O$ complex detected no free Cu(II) ions in solution leading us to conclude that the major impurity in solution is the $Cu(2\text{-}MeIm)_2^{2+}$ complex. Otherwise, EDTA is possibly reacting with any Cu(II)-hydroxy species that exists in solution.

Previous studies on copper-peroxy interactions had reported a free radical type mechanism with the hydroxyl radical ($^{\cdot}OH$) playing a major role [10-12]. An example of such a free radical mechanism is that proposed by Meyerstein, D. [22];

$^{\cdot}CH_2OH + Cu^{2+}(aq) \longrightarrow CH_2O + H_3O^+ + Cu^+(aq)$ (35)

$Cu^+ (aq) + H_2O_2 \longrightarrow Cu^{2+} (aq) + OH^- + OH$ (36)

$^{\cdot}OH + CH_3OH \longrightarrow H_2O + {}^{\cdot}CH_2OH$ (37)

$Cu^{3+}(aq) + CH_3OH \longrightarrow Cu^{2+}(aq) + CH_2OH + H^+$ (38)

Methanol is a good hydroxyl radical scavenger and should affect the rate of decomposition of hydrogen peroxide if it proceeds via a free radical pathway. When some methanol was injected into a solution containing CuB_2 followed by the addition of microliter amounts of hydrogen peroxide, no noticeable change in rate, or the 445 nm peak intensity relative to the methanol-free spectrum was observed. This leads us to the conclusion that the reaction does not proceed via a free radical pathway.

In order to verify that copper remained in the +2 state after catalyzing the reaction involving the decomposition of hydrogen peroxide into water and oxygen, two pieces of evidence were used. The CuB_2/H_2O_2 solution spectra before and after one hour of elapsed time were compared to see if the peak intensity for the 595 nm d-d absorption transition remained constant at the end of the reaction. It was observed that there was no shift or disappearance of the 595 nm peak characteristic of d^9 (Cu(II)) and not d^{10} (Cu(I)) complexes. Solutions of CuB_2/H_2O_2 or CuB_2/EDTA/H_2O_2 were tested with 2,2'-biquinoline after two hours of elapsed time and checked to see if the solution turned pink which was indicative of the fact that Cu(II) had been reduced to Cu(I). No definite pink color was observed during the time course of the testing. Both the spectroscopic and qualitative tests point to an unchanged +2 oxidation state of copper ion.

In conclusion, a valuable contribution to the copper-peroxy and Cu/O_2 interactions has been made. Molecular weight determinations have confirmed the previously reported dimeric structure of $[CuSALAD]_2.H_2O$, which reacts with imidazole bases in a 1 : 4 stoichiometric ratio.

The decomposition of hydrogen peroxide by CuSALAD.B_2 has been studied. Two spectrally active intermediates have been characterized and the effects of EDTA and $Cu(NO_3)_2$ on the rate the rate of decomposition of hydrogen peroxide have been studied. The fitting of data obtained via the isolation method has been used to attempt a study of the overall rate of decomposition of hydrogen peroxide through a non- free radical mechanism without the reduction of copper(II) to copper(I). The pH effects of the different imidazoles were studied in acidic, neutral, and basic pH ranges.

The study of such inorganic models has paved the way for future studies such as correlating the stability of Cu(II)-B complexes to that of Cu(II) catalase activity to enhance Cu/protein chemistry, studying reactions involving both the dimer and monomer in hydrous and anhydrous forms. It would also be worthwhile to completely understand the effect of EDTA and how the impurities can be removed prior to any kinetic studies. Computational calculations can be used to investigate the possible Cu/O_2 intermediates by calculating 'Reaction thermodynamics and potential surfaces'. Density functional calculations using Gaussian 98, B3LYP functional at the spin-unrestricted level have been previously done for different ligands and bases [23].

BIBLIOGRAPHY

1. Ross, P. K; and Solomon, E. I., *J. Am. Chem. Soc.*, **1991**, *113*, 3246-3259.

2. Shin, W., Sundaram, U. M., Cole, J. L., Zhang, H. H., Hedman, B., Hodgson, K. O., and Solomon, E. I., *J. Am. Chem. Soc.*, **1996**, *118*, 3202-3215.

3. Brown, J. C. and Wardeska, J. G., *Inorg. Chem.*, **1982**, *21*, 1530-1534.

4. Fawcett, T. G., Bernarducci, E. E., Krogh-Jespererersen, K., and Schugar, H. J., *J. Am. Chem. Soc.*, **1980**, *102*, 2598.

5. John D. Davis Jr., *MS Thesis*, Dept. of Chem. East TN. State Uni, **2003** p. *38*.

6. Schubert, J. and Sharma, V. S., *J. Am Chemical Society.*, **1969**, *91* 8291-8296.

7. Jiang, F., Karlin, K. D., and Peisach, J., *Inorg. Chem.*, **1993**, *32*, 2576-2582.

8. J. P. Klinman, *Chem. Rev.***1996**, *96*, 2541

9. E. I. Solomon, U. M. Sundaram, T. E. Machonkin, *Chem. Rev.* **1996**, *96*, 2563

10. V. M. Berdinov. Zh. Fiz., *Khim*. *47* (1973), 1879

11. K. V. Ponganis, M.A. De Araujo, H.L. Hodges, *Inorg. Chem* **1980**, *19*, 2704

12. G. R. A. Johnson, N. B. Nazhat, R. A. Sadalla-Nazhat, *J. Chem. Soc.*, *Chem-Commun.*, (**1985**), *407*.

13. Y. Luo, K. Kustin, I. R., Epstein, *Inorg. Chem*. **1988**, *27*, 2489.

14. Principles of Physical Chemistry, Samuel H. Mason, Carl F. Prutton, 1962, *173-189*.

15. G. Schwarzenbach and J. Heller, *Helv. Chim. Acta*, **1951**, *34*, 576.

16. M. Orhannovic and R. G. Wilkins, *Croat. Chem. Acta,* **1967**, *39*, 149.

17. V. Baran, *Coord. Chem. Rev.*, **1971**, *6*, 65.

18. G. H. Nancollas, *Coord. Chem. Rev.*, **1970**, *5,* 379.

19. J. H. Espenson, Chemical kinetics and Reaction mechanisms McGraw-Hill, New

York, **1995**, p. *105*

20. Wilkins, R. G. Kinetics and Mechanisms of Reactions of Transition Metal Complexes, 2nd Edition, **1991**, *4-21*

21. H. Ackermann, G. Shwarzenbach. Helv. *Chim. Acta*, *32*, 1543 (**1949**).

22. Meyerstein, Dein, *Inorg. Chem*. **1971**, *10*, 638

23. Peng Chen and Edward I. Solomon, *J. Chem. Soc*., **2003**, (published on web)

APPENDICES

Appendix A
Determination of $[CuSALAD]_2$/2-MeIm Stoichiometry

Volume of base (microliters)	Total volume (microliters)	ABS (595 nm)	A_{corr} for blank and dilution	2-MeIm/$[CuSALAD]_2$
0	0	0.3104	0.298	0.000
5	5	0.3267	0.318	0.1850
5	10	0.3415	0.333	0.3700
5	15	0.3491	0.347	0.5550
5	20	0.3753	0.359	0.7400
5	25	0.4045	0.372	0.9250
7.5	32.5	0.4145	0.386	1.203
7.5	40	0.4232	0.397	1.480
10	50	0.4368	0.421	1.850
25	75	0.4919	0.461	2.775
25	100	0.5193	0.498	3.544
25	125	0.5438	0.522	4.332
25	150	0.5473	0.531	5.550
50	200	0.5493	0.536	7.400
150	250	0.5478	0.538	9.250
100	350	0.5384	0.542	12.95
100	450	0.5270	0.541	16.65
200	650	0.5081	0.542	24.050

Appendix B
Effect of Varying the Imidazole Derivatives on the Rate of Hydrogen Peroxide Decomposition

$[[CuSALAD]_2.H_2O]_0 = 0.00400$ M, $[H_2O_2]_0 = 0.00130$ M, $[B] = 0.0800$ M

Time, minutes	ABS (445 nm) for 2-MeIm	ABS (448 nm) for 4-MeIm	ABS (448 nm) for ImH
0.0	0.000	0.000	0.000
0.5	0.526	0.480	0.376
1.0	0.801	0.781	0.642
2.0	1.130	1.067	0.960
3.0	1.584	1.241	1.115
5.0	1.796	1.402	1.209
7.0	1.789	1.443	1.218
10.0	1.642	1.402	1.187
12.5	1.491	1.332	1.121
15.0	1.345	1.235	1.028
17.5	1.201	1.117	0.891
20.0	1.082	0.991	0.778
25.0	0.933	0.857	0.631
30.0	0.741	0.675	0.489
35.0	0.566	0.503	0.375
40.0	0.441	0.397	0.275
45.0	0.355	0.286	0.201
50.0	0.282	0.201	0.155
55.0	0.224	0.139	0.102
60.0	0.164	0.096	0.081

Appendix C
Absorbance *vs.* Time Data for the Decomposition of Hydrogen Peroxide at 445 nm as [H_2O_2] is Varied

$[CuSALAD.2\text{-}MeIm]_0 = 0.0040$ M

Time, minutes	ABS(445 nm) for 0.00045 M H_2O_2	ABS (445 nm) for 0.0013 M H_2O_2	ABS (445 nm) for 0.0022 M H_2O_2
0.00	0.000	0.000	0.000
0.5	0.387	0.479	0.568
1.0	0.473	0.648	0.803
1.5	0.546	0.774	1.152
2.0	0.593	0.868	1.261
2.5	0.612	0.932	1.337
3.0	0.647	1.021	1.372
3.5	0.668	1.056	1.415
4.0	0.694	1.112	1.422
4.5	0.703	1.142	1.448
5.0	0.723	1.151	1.463
7.5	0.741	1.162	1.460
10.0	0.725	1.133	1.409
12.5	0.714	1.122	1.372
15.0	0.701	1.113	1.347
17.5	0.684	1.096	1.321
20.0	0.673	1.071	1.282
25.0	0.629	1.032	1.241
30.0	0.604	0.996	1.178
35.0	0.583	0.910	1.126
40.0	0.552	0.861	1.057
50.0	0.518	0.802	0.975
60.0	0.473	0.724	0.908
70.0	0.437	0.658	0.811
80.0	0.383	0.601	0.723

Appendix D
Absorbance *vs*. Time Data showing the Effect of Varying [[CuSALAD]$_2$.H_2O] on the Rate of Peroxide Decomposition

[[CuSALAD]$_2H_2O$]$_0$ = 0.00400 M, [H_2O_2]$_0$ = 0.00440 M, [2-MeIm]$_0$ = 0.0800 M

Time, minutes	Abs (445nm) 0.00267 M	Abs (445nm) 0.00191 M	Abs(445nm) 0.00114 M	Abs (445nm) 0.000381 M
0.0	0.000	0.0000	0.0000	0.0000
0.2	0.3352	0.2216	0.2133	0.1869
0.4	0.5526	0.4879	0.4045	0.3544
0.6	0.7012	0.6634	0.5654	0.5264
1.0	0.9923	0.9887	0.8335	0.8012
1.5	1.2715	1.2246	1.1332	1.1132
2.0	1.4565	1.4678	1.3341	1.3021
3.0	1.6747	1.7103	1.5789	1.5843
4.0	1.7985	1.8204	1.7032	1.7321
5.0	1.8112	1.8822	1.7341	1.7963
6.0	1.7862	1.8726	1.7465	1.8126
7.0	1.7448	1.8224	1.7112	1.7896
8.0	1.6697	1.7338	1.6422	1.7423
9.0	1.6123	1.6985	1.6249	1.6896
10.0	1.5561	1.6539	1.5849	1.6423
12.5	1.4236	1.4475	1.4032	1.4913
15.0	1.2574	1.3139	1.2654	1.3436
17.5	1.1365	1.2285	1.1346	1.2021
20.0	1.0987	1.149	1.0987	1.0367
22.5	0.9736	1.0679	0.9872	0.9897
25.0	0.8887	0.9018	0.9029	0.9332
27.5	0.7723	0.8329	0.8285	0.8339
30	0.6778	0.7267	0.7236	0.7413
32.5	0.5939	0.6365	0.6281	0.6275
35.0	0.5345	0.5746	0.5689	0.5664
40.0	0.4096	0.4876	0.4658	0.4412
45.0	0.3455	0.4013	0.3895	0.3546
50.0	0.2829	0.3341	0.3031	0.2824
55.0	0.2231	0.2678	0.2542	0.2242
60.0	0.1789	0.1879	0.1988	0.1641

Appendix E

Absorbance *vs*. Time Data showing the Rate of Peroxide Decomposition in the Absence and Presence of EDTA**.**

$[[CuSALAD]_2]_0$=0.00400 M, $[2\text{-}MeIm]_0$=0.0800 M, $[EDTA]_0$=0.00240 M, $[H_2O_2]_0$=0.00130 M

Time, minutes	CuSALAD.2-MeIm/H_2O_2 Abs (peak at 445 nm)	CuSALAD.2-MeIm.EDTA/H_2O_2 abs (peak at 445 nm)
1.000	1.6221	0.1054
1.500	1.6264	0.1745
2.000	1.6193	0.2266
2.500	1.6096	0.2797
3.000	1.5597	0.3229
3.500	1.5093	0.3684
4.000	1.4887	0.4054
5.000	1.3958	0.4784
10.000	0.9904	0.7604
15.000	0.6741	0.9718
20.000	0.4294	1.1440
25.000	0.2958	1.2695
30.000	0.2105	1.3373
35.000	0.1565	1.3486
40.000	0.1057	1.3032
45.000	0.1020	1.2000
50.000	0.0750	1.0490
55.000	0.0520	0.8742
60.000	0.0391	0.7008

Appendix F
The Effect of pH on the Rate of Peroxide Decomposition

$[[CuSALAD]_2]_0 = 0.00400$ M, $[2\text{-MeIm}]_0 = 0.0800$ M)

Time, minutes	pH 6.5 (Abs peak at 445 nm)	pH 7.7 (Abs peak at 445 nm)	pH 8.5 (Abs peak at 445 nm)
0.000	0.2231	0.2861	0.2604
1.500	0.4407	1.1509	0.4117
3.000	0.7032	1.3536	0.5531
4.500	0.8515	1.4907	0.7409
6.000	0.8847	1.7526	0.8526
7.500	0.8432	1.9881	1.0831
10.00	0.7314	1.8434	1.1323
12.00	0.6252	1.7225	1.1814
14.00	0.5509	1.6032	1.1905
16.00	0.4832	1.2518	1.1727
20.00	0.4191	0.8104	1.0604
30.00	0.3323	0.6233	0.5413
40.00	0.3012	0.5414	0.4408
60.00	0.2918	0.4828	0.4210
80.00	0.2907	0.4231	0.3883
100.0	0.2838	0.4015	0.3861
120.0	0.2814	0.3705	0.3807

Appendix G
Comparison of the Rate of Decomposition of Hydrogen Peroxide by CuSALAD.B_2 in the Presence of Copper(II) nitrate

Time, minutes	ABS(445 nm) for CuSALAD.B_2 (0.00400 M)	ABS(445 nm) for both CuSALAD.B_2 and 0.00200 M Cu(II) nitrate
0.0	0.000	0.000
0.3	1.636	1.823
0.6	1.774	1.931
0.9	1.743	1.915
1.0	1.716	1.902
1.5	1.587	1.715
2.0	1.442	1.509
2.5	1.262	1.330
3.0	1.117	1.206
4.0	0.912	1.003
5.0	0.729	0.812
6.0	0.591	0.626
8.0	0.386	0.475
10.0	0.270	0.364
12.0	0.191	0.253
14.0	0.150	0.209
16.0	0.124	0.165
18.0	0.109	0.137
20.0	0.101	0.116

Appendix H
Investigation of the Effect of MeOH on the Rate of Decomposition of Hydrogen Peroxide

Time, minutes	Abs (445 nm), no MeOH 0.00400 M $Cu(2\text{-}MeIm)_2$	Abs (445 nm) with MeOH 0.00400 M CuB_2 + 0.00200 M MeOH
0.00	0.0004	0.0002
0.50	0.7250	0.7271
1.00	0.9984	0.9573
1.50	1.1931	1.1320
2.00	1.3450	1.2701
2.50	1.4556	1.3787
3.00	1.5384	1.4642
4.00	1.6394	1.5790
5.00	1.6877	1.6436
10.00	1.6806	1.6695
15.00	1.5127	1.5213
20.00	1.2562	1.2803
25.00	0.9801	1.0029
30.00	0.7267	0.7413
35.00	0.5203	0.5263
40.00	0.3640	0.3627
45.00	0.2484	0.2455
50.00	0.1688	0.1657
55.00	0.1178	0.1146

VITA

TIMOTHY KUM BENG

Personal Data:	Date of Birth: April 02, 1979
	Place of Birth: Lobe Estate, Ekondo-titi, Cameroon
	Marital Status: Single
	Nationality: Cameroonian
Education:	Government Bilingual High School, Ekondo-titi, 1991 - 1996
	St. Bedes College, Ashing, 1996 – 1998: High School Diploma
	University of Buea, 1998 - 2001; BSc. Chemistry.
	East Tennessee State University, 2003 – 2004, MS Chemistry
Experience:	President of Buea University Chemical Society, 2000-2001
	Soccer Player-Manager, Green Eagles Yaoundé, 2001-2002
	Lab Instructor, East Tennessee State University, 2003-Present
Skills:	Instrument Operation, UV-Vis, IR, NMR Spectrometers.
	MS-Word, Excel, PSI Plot, Derive, PC Model, Spartan,
	Gaussian, Scientist, Chem. Draw.
Hobbies:	Soccer, Music, Eating Chinese food.
Awards:	Chemistry Departmental Prize for Best Graduating Student, University of Buea, Cameroon, 2001.
	Guinness Cameroon's Prize for Second Outstanding Graduating Student, University of Buea, Cameroon, 2001.
References:	University of Buea, P. O. Box 63, Buea, Cameroon East Tennessee State University, Johnson City, Tennessee.